Supporting Information for

Unusual cyanide and methyl binding modes at a dicobalt macrocycle following acetonitrile C–C bond activation

Ariana Z. Spentzos, Michael R. Gau, Patrick J. Carroll, Neil C. Tomson*

P. Roy and Diana T. Vagelos Laboratories, Department of Chemistry, University of Pennsylvania, Philadelphia, Pennsylvania 19104, United States

Table of Contents:

General Considerations: S2

Experimental Procedures and Characterization Data: S4

NMR Spectra: S9

IR Spectra: S28

UV-Vis Spectra: S32

Cyclic Voltammogram: S34

X-ray Crystallography: S35

References: S41

General Considerations

All reactions containing transition metals were performed under an inert atmosphere of N_2, using standard Schlenk line or glovebox techniques. Glassware, stir bars, filter aid (Celite), and 3 Å molecular sieves were dried in an oven at 150 °C for at least 12 h prior to use. All solvents (THF, pyridine, acetonitrile, fluorobenzene, 1,2-difluorobenzene, *n*-pentane and diethyl ether) were dried by passage through a column of activated alumina, deoxygenated by passage through a copper Q5 column where applicable, sparged with N_2, and stored over activated 3 Å molecular sieves under an inert atmosphere. Deuterated solvents were purchased from Cambridge Isotope Laboratories, Inc., and dried over either Na/benzophenone (THF-d_8, C_6D_6) or CaH_2 (MeCN-d_3), isolated by vacuum transfer (THF-d_8, MeCN-d_3) or distillation (C_6D_6), and stored under an inert atmosphere over 3 Å sieves. **[^{3}PDI$_2$Co$_2$(μ-Cl)(PMe$_3$)$_2$][OTf] ([Co$_2$Cl]$^+$)** was synthesized following previously published procedures.[1] KC_8 was synthesized according to a literature procedure[2] and stored under nitrogen at −35 °C in a glovebox prior to use. PMe_3 (98%) was either purchased from Strem Chemicals or synthesized according to a literature procedure;[3] in both cases, it was stored as a 1 M solution in THF at −35 °C under dry nitrogen in a glovebox over 3 Å molecular sieves. $NaBAr^F{}_4$ was prepared according to a literature procedure.[4] $K^{13}CN$ and $^{13}CH_3CN$ were purchased from Sigma Aldrich and both NaCN and $K^{13}CN$ were ground to fine powders before use. Methylmagnesium chloride solution (3.0 M in THF) was purchased from Sigma Aldrich and titrated using salicylaldehyde phenylhydrazone.[5] [^{n}Bu$_4$N][PF$_6$] (98%) was purchased from MilliporeSigma and recrystallized twice from hot ethanol, followed by drying at 60 °C under 30 mbar for 10 h and stored in a glovebox under dry nitrogen prior to use.[6] Ferrocene (98%) was purchased from Acros Organics, purified by sublimation three times,[7] and stored in a glovebox under dry nitrogen prior to use. All other chemicals were used as received. ^{1}H, ^{13}C{^{1}H}, ^{31}P{^{1}H}, ^{19}F{^{1}H}, ^{1}H–^{13}C HSQC, ^{1}H–^{13}C HMBC, and ^{1}H–^{1}H COSY NMR spectra were recorded on UNI 400, UNI 500, Bruker BioDRX500, Cryo 500, and NEO 600 spectrometers. All chemical shifts (δ) are reported in units of ppm, with references to the residual protio-solvent resonance for proton and carbon chemical shifts. External H_3PO_4 was used for referencing ^{31}P NMR spectra. Internal PhF was used for referencing ^{19}F NMR spectra.[8] For the complexes with asymmetry in the PDI signals, the apostrophes in the assignments given below refer to the portion of the ligand closest to the coordinated PMe_3. Elemental analysis was performed by Midwest Microlab, LLC. IR spectra (KBr pellet) were collected on a JASCO FT/IR-480 Plus spectrometer FTIR. Solution phase effective magnetic moment data were determined using Evans' method.[9]

Cyclic voltammetry experiments were performed in a VAC OMNI-LAB glovebox with an Epsilon E2 Potentiostat. The data were processed with BASi Epsilon-EC software version 2.13.77. All experiments were performed under an N_2 atmosphere in a glovebox using an electrochemical cell that consists of a glassy carbon (3 mm outer diameter) working electrode, a platinum wire counter electrode, and a Ag/$AgBAr^F{}_4$ (1 M in 1,2-difluorobenzene) reference electrode. All experiments were conducted in 1,2-difluorobenzene, with 1 mM analyte and 100 mM [^{n}Bu$_4$N][PF$_6$] as the supporting electrolyte. Potentials were reported versus $Cp_2Fe^{+/0}$.

UV−vis−NIR absorption spectra were collected from 200 to 1000 nm using an Agilent Cary 60 UV−vis spectrophotometer at room temperature. The samples were prepared under an N_2 atmosphere in a glovebox. Stock solutions were prepared by dissolving a known mass (*ca*. 10

mg) of sample in 10.00 mL of solvent (**$[Co_2CN]^+$** (THF); **$[Co_4(CN)_2][OTf]_2$** and **$[Co_2CN]^{2+}$** (CH_3CN)). Varying amounts of the stock solutions (50.0−400.0 μL) were then diluted to 5.00 mL and transferred to a 10 mm path-length quartz cuvette with a screw cap for data collection. For each species, at least four spectra at different concentrations were collected. The absorption intensities of various peak maxima were plotted vs. concentration to ensure that absorption data were being collected in the linear response range of the spectrometer. Linear regression fits to the plotted data resulted in R^2 values ≥ 0.994.

Crystallographic X-ray intensity data were collected on a Bruker D8QUEST CMOS (**$[Co_4(CN)_2][BAr^F{}_4]_2$, $[Co_4(CN)_2][OTf]_2$**) or a Bruker APEXII CCD (**$[Co_2CN]^+$**, **$[Co_2CH_3]^+$**) area-detector diffractometer with graphite-monochromated Mo K_α radiation (λ = 0.71073 Å) at 100 K. X-ray intensity data for **$[Co_2CN]^{2+}$** were collected on a Rigaku XtaLAB Synergy-S diffractometer equipped with an HPC area detector (Dectris Pilatus3 R 200K) and employing confocal multilayer optic-monochromated Mo-K_α radiation (λ=0.71073 Å) at a temperature of 100 K. Rotation frames were integrated using SAINT[10] or CrysAlisPro[11] (**$[Co_2CN]^{2+}$**) producing a listing of unaveraged F^2 and $\sigma(F^2)$ values. The intensity data were corrected for Lorentz and polarization effects and for absorption using SADABS[12] or SCALE3 ABSPACK[13]. The structures were solved by direct methods by using either SHELXT[14] (**$[Co_2CN]^+$**, **$[Co_4(CN)_2][BAr^F{}_4]_2$**, **$[Co_4(CN)_2][OTf]_2$**, **$[Co_2CN]^{2+}$**) or SHELXS-97[15] (**$[Co_2CH_3]^+$**) and refined by full-matrix least-squares, based on F^2 using SHELXL-2018.[16] For **$[Co_4(CN)_2][OTf]_2$**, a reliable disorder model could not be devised for the triflates; the X-ray data were corrected for the presence of disordered triflates using SQUEEZE.[17] For **$[Co_2CN]^+$**, there are two independent molecules, each of which lies on a crystallographic mirror plane. Molecule No.1 lies parallel to the mirror plane that passes through the atoms Co1, Co2, N5/C5*, C6*/N6, N3, C5, C17, N2, C4, C13. Analysis of the thermal parameters led to the conclusion that the two linking atoms are 50/50 C/N mixtures. Molecule No. 2 is perpendicular to the mirror plane, which bisects the C4"/N4'-N4'/C4" bond. The linking pair of atoms in this molecule are required by symmetry to be identical. Therefore, they are each a 50/50 C/N mixture. For **$[Co_2CN]^{2+}$**, the molecule lies on a crystallographic 2-fold axis (at ½, y, ¼) that bisects the Co-Co vector and disorders the coordinated cyanide so that half the molecules have it bonded to one Co and half the molecules have it on the other. For **$[Co_2CH_3]^+$**, hydrogen atoms were refined using a riding model, except for the H's on the bridging carbon, C36, which were refined isotropically. CCDC entries 2002336-2002338, 2002340 contain the supplementary crystallographic data for this paper. These data can be obtained free of charge from the Cambridge Crystallographic Data Centre via www.ccdc.cam.ac.uk/ data_request/cif.

Experimental Procedures and Characterization Data

Synthesis of [(^{3}PDI$_2$)Co$_2$(μ-CH$_3$)(PMe$_3$)][OTf] ([Co$_2$CH$_3$]$^+$)

Method A: A 20 mL scintillation vial was charged with **[Co$_2$Cl]$^+$** (23.1 mg, 0.02 mmol, 1.0 equiv), acetonitrile (23.5 µl, 0.508 M in THF, 0.01 mmol, 0.5 equiv) and 3 mL of THF. The dark green solution was frozen in a liquid nitrogen chilled cold-well. KC_8 (3.4 mg, 0.025, 1.1 equiv) was quickly added in one aliquot to the thawing solution, which turned blue-black before turning back to green upon warming. After stirring for 3 minutes, the solvent was removed *in vacuo* and the green solid was extracted into THF (3 mL) and filtered through Celite. The THF was removed *in vacuo* and a crude green solid (18.4 mg) was analyzed spectroscopically. NMR spectroscopic yields of **[Co$_2$CH$_3$]$^+$** ranged from 33%-43% with **[Co$_2$CN]$^+$** (17%) and **[Co$_4$(CN)$_2$][OTf]$_2$** (4%) accounting for the remaining diamagnetic products. Small amounts of crystalline **[Co$_2$CH$_3$]$^+$** and **[Co$_2$CN]$^+$** were repeatedly isolated from PhF/pentane vapor diffusion crystallizations. PMe_3 was added to favor crystallization of **[Co$_2$CN]$^+$**. Repeated crystallizations without added PMe_3 gave higher purity fractions of **[Co$_2$CH$_3$]$^+$**.

Method B: A 20 mL scintillation vial was charged with **[Co$_2$Cl]$^+$** (66.0 mg, 0.07 mmol, 1.0 equiv) and *ca*. 2 mL THF. A dilute solution of MeMgCl (22.7 µL, 3.0 M in THF, 0.07 mmol, 1.0 equiv; diluted to 8 mL in THF) was added dropwise over 10 minutes at ambient temperature with vigorous stirring. The solution gradually turned dark blue and was stirred for 1 minute following addition of MeMgCl. The solvent was removed *in vacuo*, and the solid was washed with ether (3 x 5 mL). Attempted crystallizations from this method failed to give isolable crystalline product, but NMR spectral analysis of the solid revealed the material to be the same as that isolated through Method A. The product decayed over several hours with loss of methane, as observed by NMR spectroscopy; no such decomposition was observed with product synthesized from Method A. When PMe_3 was added to material synthesized through Method B, broader and symmetric peaks were observed, and minimal decomposition was observed; however, this product has not been isolated.

^{1}H NMR (500 MHz, THF-d_8, 300 K) δ 7.45 (s, 2H, py' *m*-H), 7.40 (s, 2H, py *m*-H), 3.73 (ddd, $^2J_{HH}$ = 12.8, $^3J_{HH}$ = 4.5, $^3J_{HH}$ = 2.6 Hz, 2H, CH$_2$CH$_2$C'*H*$_2$), 3.55-3.42 (m, 6H, C*H*$_2$CH$_2$C'H$_2$ (4H) and CH$_2$CH$_2$C'*H*$_2$ (2H) overlapped), 2.59 (m, 2H, CH$_2$C*H*$_2$C'H$_2$), 2.25 (d, $^5J_{PH}$ = 6.7 Hz, 6H, N=C-C'*H*$_3$), 1.95 (dt, *J* = 14.8, 3.0 Hz, 2H, CH$_2$C*H*$_2$C'H$_2$), 1.81 (s, 6H, N=C-C*H*$_3$), 1.26 (s, 9H, C(C*H*$_3$)$_3$), 1.19 (s, 9H, C(C'*H*$_3$)$_3$), 1.04 (d, $^2J_{PH}$ = 8.2 Hz, 9H, P(C*H*$_3$)$_3$), -3.22 (s, 3H, C*H*$_3$) ppm.

^{13}C{^{1}H} NMR (126 MHz, THF-d_8, 300 K) δ 155.1 (d, $^3J_{PC}$ = 7.1 Hz, C'$_{imine}$), 150.1 (s, C$_{imine}$), 148.4 (s, *o*-Ar*C)*, 148.3 (d, $^3J_{PC}$ = 3.2 Hz, *o*-Ar*C'*), 146.1 (d, $^5J_{PC}$ = 3.3 Hz, *p*-Ar*C'*), 143.7 (s, *p*-Ar*C*), 117.7 (d, $^4J_{PC}$ = 1.9 Hz, *m*-Ar*C'*), 113.8 (s, *m*-Ar*C*), 55.3 (s, CH$_2$CH$_2$*C*'H$_2$), 53.9 (s, *C*H$_2$CH$_2$C'H$_2$), 36.2 (s, *C*(CH$_3$)$_3$), 35.8 (s, *C'*(CH$_3$)$_3$), 32.5 (d, $^4J_{PC}$ = 4.1 Hz, CH$_2$*C*H$_2$C'H$_2$), 31.4 (s, C(*C'*H$_3$)$_3$), 31.2 (s, C(*C*H$_3$)$_3$), 14.6 (d, $^1J_{PC}$ = 18.3 Hz, P(*C*H$_3$)$_3$), 14.6 (s, N=C-*C*H$_3$), 14.0 (d, $^4J_{PC}$ = 3.6 Hz, N=C-*C'*H$_3$) ppm. The bridging *C*H$_3$ resonance was not identified in this spectrum; see below.

^{31}P{^{1}H} NMR (162 MHz, THF-d_8, 300 K): δ = -2.06 (s, *P*(CH$_3$)$_3$) ppm.

The ^{13}C enriched isotopologue **$[Co_2{}^{13}CH_3]^+$** was synthesized as described above in Method A using neat $^{13}CH_3CN$. Selected data for **$[Co_2{}^{13}CH_3]^+$**:

^{13}C NMR (126 MHz, THF-d_8, 300 K): δ = 12.4 (q, $^1J_{CH}$ = 110.0 Hz, Co-CH_3) ppm.

^1H NMR (500 MHz, THF-d_8, 220 K) δ = -12.7 (d, $^1J_{CH}$ = 74.5 Hz, 1H, Co-CH_3) ppm.
$^{13}C\{^1H\}$ NMR (126 MHz, THF-d_8, 220 K): δ = 14.9 (s, Co-CH_3) ppm.

Repeated recrystallizations failed to yield analytically pure **$[Co_2{}^{13}CH_3]^+$**.

Synthesis of $[(^3PDI_2)Co_2(\mu\text{-}CN)(PMe_3)_2][OTf]$ ($[Co_2CN]^+$)
Method A: See Method A of **$[Co_2CH_3]^+$** for synthesis of **$[Co_2CN]^+$** from MeCN.

Method B: A flask was charged with **$[Co_2Cl]^+$** (82.8 mg, 0.09 mmol, 1.0 equiv), NaCN (4.4 mg, 0.09 mmol, 1.0 equiv), and *ca.* 3 mL of pyridine. The dark green solution was stirred at 95 °C for 2 days. The solution gradually turned dark green-brown. The solvent was removed *in vacuo* and the solid was twice triturated with pentane. The solid was then extracted with fluorobenzene (~5 mL) and filtered through Celite. One drop of PMe_3 was added to the solution. Layering with pentane (10 mL) afforded blocks of **$[Co_2CN]^+$** (55 mg, 59%) after 3 d at ambient temperature.

^1H NMR (500 MHz, THF-d_8, 300 K): δ = 7.79 (s, 4H, py *m*-H), 4.60-4.54 (br q, 4H, $CH_2CH_2CH_2$), 3.80-3.76 (br t, 4H, $CH_2CH_2CH_2$), 2.55-2.47 (m, 2H, $CH_2CH_2CH_2$), 2.18 (d, $^5J_{PH}$ = 9.6 Hz, 12H, N=C-CH_3), 1.42 (m, overlapped, 2H, $CH_2CH_2CH_2$), 1.39 (s, 18H, $C(CH_3)_3$), 0.89 (d, $^2J_{PH}$ = 9.4 Hz, 18H, $P(CH_3)_3$ ppm.

$^{13}C\{^1H\}$ NMR (126 MHz, THF-d_8, 300 K): δ = 170.4 (s, $C{\equiv}N$), 153.0 (d, $^3J_{PC}$ = 5.4 Hz, C_{imine}), 147.8 (s, *o*-Ar*C*), 142.9 (d, $^5J_{PC}$ = 10.1 Hz, *p*-Ar*C*), 119.1 (d, $^4J_{PC}$ = 5.8 Hz, *m*-Ar*C*), 58.1 (s, $CH_2CH_2CH_2$), 36.4 (s, $C(CH_3)_3$ and $CH_2CH_2CH_2$), 31.0 (s, $C(CH_3)_3$), 13.8 (s, N=C-CH_3), 13.3 (d, $^1J_{PC}$ = 16.9 Hz, $P(CH_3)_3$) ppm.

$^{19}F\{^1H\}$ NMR (376 MHz, THF-d_8, 300 K): δ = −78.7 (s, CF_3) ppm.

$^{31}P\{^1H\}$ NMR (162 MHz, THF-d_8, 300 K): δ = 29.7 (s, $P(CH_3)_3$) ppm.

Anal. Calcd. for $C_{40}H_{64}Co_2F_3N_7O_3P_2S_1$ • 1 $C_6H_5F_1$ and ½ C_5H_{12} (1092.0 g/mol): C, 53.34; H, 6.92; N, 8.98. Found: C, 53.24; H, 7.03 ; N, 8.87 %.

IR (KBr): ν_{CN} = 2098 cm^{-1}

UV-vis-NIR (THF): 265 nm (4.28×10^4 M^{-1} cm^{-1}), 420 nm (2.10×10^4 M^{-1} cm^{-1}), 561 nm (4.29×10^3 M^{-1} cm^{-1}) and 879 nm (3.73×10^3 M^{-1} cm^{-1}).

The ^{13}C enriched isotopologue **$[Co_2{}^{13}CN]^+$** was synthesized as described above, using $K^{13}CN$ as the cyanide source. Selected data for **$[Co_2{}^{13}CN]^+$**: IR (KBr): ν_{CN} = 2054 cm^{-1}

Synthesis of $[(^3PDI_2)Co_2(\mu\text{-}CN)(PMe_3)_2][OTf]_2$ ($[Co_2CN]^{2+}$)
$[Co_2CN]^+$ (29.5 mg, 0.03 mmol, 1.0 equiv) was added to a 20 mL scintillation vial and dissolved in THF (3 mL). AgOTf (6.9 mg, 0.03 mmol, 1.0 equiv) was dissolved in minimal THF and added to the stirring dark green solution in one aliquot at ambient temperature. Immediate formation of a dark precipitate and a metallic coating on the walls of the flask were observed. The reaction was stirred for 5 minutes before removal of the solvent *in vacuo*. The dark green solid was washed with THF (1 mL), extracted with 1,2-difluorobenzene (*ca*. 2 mL) and filtered through Celite. Vapor diffusion of pentane into the 1,2-difluorobenzene solution overnight yielded dark green-brown thick plates (22.1 mg, 74%).

^{1}H NMR (400 MHz, MeCN-d_3, 300 K): δ = 18.2 (br s), 11.1 (br s), 1.4 (s, C(CH_3)$_3$), -7.6 (br s) ppm.

Anal. Calcd. for $C_{41}H_{64}Co_2F_6N_7O_6P_2S_2$ (1108.93 g/mol): C, 44.41; H, 5.82; N, 8.84. Found: C, 44.21; H, 5.69 ; N, 8.35 %.

IR (KBr): ν_{CN} = 1975 cm^{-1}

UV-vis-NIR (MeCN): 234 nm (3.75 × 10^4 M^{-1} cm^{-1}), 288 nm (shoulder, 1.39 × 10^4 M^{-1} cm^{-1}), 416 nm (9.81 × 10^3 M^{-1} cm^{-1}), 680 nm (4.61 × 10^3 M^{-1} cm^{-1}), 852 nm (6.65 × 10^3 M^{-1} cm^{-1}).

Synthesis of $[(^3PDI_2)_2Co_4(\mu\text{-}CN)_2(PMe_3)_2][OTf]_2$ ($[Co_4(CN)_2][OTf]_2$)
A heavy-walled glass vessel was charged with **$[Co_2Cl]^+$** (248.5 mg, 0.26 mmol, 1.0 equiv), NaCN (12.6 mg, 0.26 mmol, 1.0 equiv), and *ca.* 5 mL of pyridine. The dark green solution was stirred at 95 °C for 5 days. The solution gradually turned dark green-brown. The solvent was removed *in vacuo* and the solid was twice triturated with pentane. The dark green solid was extracted with THF (6 x 2 mL) and filtered through Celite. The remaining purple solid (after extraction of **$[Co_2CN]^+$**) was extracted with 1,2-difluorobenzene (*ca.* 6 mL), filtered through Celite, and layered with pentane (*ca.* 10 mL). After an additional recrystallization under the same conditions, **$[Co_4(CN)_2][OTf]_2$** was isolated as dark purple blocks (60.1 mg, 27%).

The solution-phase dynamics and low solubility of **$[Co_4(CN)_2][OTf]_2$** prevented the collection of a full complement of NMR spectral data, but comparison of the observables with those for **$[Co_4(CN)_2][BAr^F{}_4]_2$** support the assigned structure.
^{1}H NMR (500 MHz, 1,2-difluorobenzene-h_4/C_6D_6): δ 7.32 (s, 4H, py *m*-H), 6.95 (s, 4H, py' *m*-H), 6.03 (dd, *J* = 14.7, 11.8 Hz, 4H, CH_2CH$_2$C'H$_2$), 4.94 – 4.56 (m, 4H, CH$_2$CH$_2$C'H_2), 4.17 (br d, *J* = 12.7 Hz, 4H, CH$_2$CH$_2$C'H_2), 4.12 – 4.04 (m, 4H, CH_2CH$_2$C'H$_2$), 3.41 – 3.26 (m, 4H, CH$_2$CH_2C'H$_2$), 2.42 (br d, *J* = 15.5 Hz, 4H, CH$_2$CH_2C'H$_2$), 2.25 (d, $^5J_{PH}$ = 8.8 Hz, 12H, N=C-C'H_3), 1.27 (s, 12H, N=C-CH_3), 1.21 (s, 18H, C(CH_3)$_3$), 0.99 (s, 18H, C(C'H_3)$_3$), 0.22 (d, $^2J_{PH}$= 9.5 Hz, 18H, P(CH_3)$_3$) ppm.

^{31}P{^{1}H} NMR (162 MHz, 1,2-difluorobenzene-h_4/C_6D_6, 300 K): δ = 3.40 (s, *P*(CH$_3$)$_3$) ppm.

Anal. Calcd. for $C_{74}H_{110}Co_4F_6N_{14}O_6P_2S_2$ (1752.54 g/mol): C, 50.28; H, 6.27; N, 11.09. Found: C, 46.70 ; H, 5.81 ; N, 11.01. Repeated attempts to generate analytically pure material were unsuccessful.

IR (KBr): ν_{CN} = 2061 cm^{-1}

UV-vis-NIR (MeCN): 245 nm (7.19×10^4 M^{-1} cm^{-1}), 318 nm (shoulder, 2.47×10^4 M^{-1} cm^{-1}), 379 nm (2.19×10^4 M^{-1} cm^{-1}), 486 nm (1.70×10^4 M^{-1} cm^{-1}), 553 nm (2.08×10^4 M^{-1} cm^{-1}).

The ^{13}C enriched isotopologue **$[Co_4(^{13}CN)_2][OTf]_2$** was synthesized as described above, using $K^{13}CN$ as the cyanide source. Selected data for **$[Co_4(^{13}CN)_2][OTf]_2$**: IR (KBr): ν_{CN} = 2020 cm^{-1}

Synthesis of $[(^3PDI_2)_2Co_4(\mu\text{-}CN)_2(PMe_3)_2][BAr^F{}_4]_2$ ($[Co_4(CN)_2][BAr^F{}_4]_2$)

A 20 mL scintillation vial was charged with **$[Co_4(CN)_2][OTf]_2$** (27.5 mg, 0.02 mmol, 1.0 equiv) and 1,2-difluorobenzene (2 mL). A solution of $NaBAr^F{}_4$ (28.8, 0.03 mmol, 2.1 equiv) in THF (*ca*. 1 mL) was added to the stirring, purple solution at room temperature. After stirring for 2 hours at ambient temperature, the solvent was removed *in vacuo*. The purple solid was triturated with pentane, washed with diethyl ether (2 x 2 mL) then extracted with THF (2 mL) and filtered through Celite. Vapor diffusion of pentane into the THF solution over 3 days at ambient temperature yielded a crop of purple needles. To remove residual NaOTf, the crystals were recrystallized from THF/pentane and twice more from fluorobenzene/pentane vapor diffusion, yielding 5.2 mg (10.5%) of the product.

^1H NMR (500 MHz, THF-d_8, 300 K): δ = 7.78 (br s, 16H, *o*-C*H* $BAr^F{}_4$), 7.57 (s, 8H, *p*-C*H* $BAr^F{}_4$), 7.54 (s, 4H, py *m*-H), 7.17 (s, 4H, py' *m*-H), 6.02-6.07 (td, *J* = 2.9 Hz, *J* = 13.4 Hz, 4H, $CH_2CH_2C'H_2$), 4.73-4.79 (td, *J* = 3.3 Hz, *J* = 13.2 Hz, 4H, $CH_2CH_2C'H_2$), 4.23-4.26 (br d, 4H, $CH_2CH_2C'H_2$), 4.14-4.19 (dt, *J* = 13.2 Hz, *J* = 3.8 Hz, 4H, $CH_2CH_2C'H_2$), 3.42-3.52 (m, 4H, $CH_2CH_2C'H_2$), 2.43 (d, $^5J_{PH}$ = 9.4 Hz, 12H, N=C-C'H_3), 2.34-2.39 (m, 4H, $CH_2CH_2C'H_2$), 1.54 (s, 12H, N=C-CH_3), 1.28 (s, 18H, $C(CH_3)_3$), 1.10 (s, 18H, $C(C'H_3)_3$), 0.37 (d, $^2J_{PH}$ = 10.0 Hz, 18H, $P(CH_3)_3$) ppm.

^1H NMR (600 MHz, 1,2-difluorobenzene-h_4/C_6D_6, 300 K): δ = 8.34-8.17 (br s, 16H, *o*-C*H* $BAr^F{}_4$), 7.55 (s, 8H, *p*-C*H* $BAr^F{}_4$), 7.36 (s, 4H, py *m*-H), 6.99 (s, 4H, py' *m*-H), 5.99 (td, *J* = 13.5, 2.9 Hz, 4H, $CH_2CH_2C'H_2$), 4.71 (td, *J* = 13.1, 3.2 Hz, 4H, $CH_2CH_2C'H_2$), 4.12-3.90 (m, 8H, $CH_2CH_2C'H_2$ and $CH_2CH_2C'H_2$ overlapped), 3.28-3.17 (m, 4H, $CH_2CH_2C'H_2$), 2.23-2.17 (m, 4H, $CH_2CH_2C'H_2$), 2.16 (d, $^5J_{PH}$ = 9.4 Hz, 12H, N=C-C'H_3), 1.24 (s, 18H, $C(CH_3)_3$), 1.19 (s, 12H, N=C-CH_3), 1.01 (s, 18H, $C(C'H_3)_3$), 0.19 (d, $^2J_{PH}$ = 9.9 Hz, 18H, $P(CH_3)_3$) ppm.

$^{13}C\{^1H\}$ NMR (126 MHz, THF-d_8, 300 K): δ = 162.8 (q, $^1J_{BC}$ =49.9 Hz, *C*-B), 153.6 (s, C_{imine}), 153.5 (d, $^3J_{PC}$ = 8.0 Hz, C'_{imine}), 149.7 (d, $^5J_{PC}$ = 7.2 Hz, *p*-Ar*C*'), 149.0 (s, *o*-Ar*C*), 148.1 (d, $^3J_{PC}$ = 2.2 Hz, *o*-Ar*C*'), 144.4 (s, *p*-Ar*C*), 135.6 (br s, *o*-*C*H $BAr^F{}_4$), 130.0 (qq, $^3J_{CB}$ = 2.8 Hz, $^2J_{CF}$ = 31.4 Hz, *m*-*C* $BAr^F{}_4$), 125.5 (q, $^1J_{CF}$ = 272.3 Hz, *C*F_3 $BAr^F{}_4$), 118.5 (d, $^4J_{PC}$ = 5.0 Hz, *m*-Ar*C'*), 118.2 (br sept, $^3J_{CF}$ = 4.0 Hz, *p*-*C* $BAr^F{}_4$), 115.5 (s, *m*-Ar*C*), 57.4 (s, $CH_2CH_2C'H_2$), 56.0 (s, $CH_2CH_2C'H_2$), 37.7 (s, $C(CH_3)_3$), 35.7 (d, $^6J_{PC}$ = 2.1 Hz, *C'*$(CH_3)_3$), 31.0 (d, $^7J_{PC}$ = 1.8 Hz,

C($C'H_3$)$_3$, 29.8 (s, C(CH_3)$_3$), 28.8 (d, $^4J_{PC}$ = 3.9 Hz, $CH_2CH_2C'H_2$), 16.5 (s, N=C-CH_3), 14.2 (d, $^4J_{PC}$ = 4.8 Hz, N=C-$C'H_3$), 11.4 (d, $^1J_{PC}$= 20.9 Hz, P(CH_3)$_3$) ppm. C≡N resonance not found.

$^{19}F\{^1H\}$ NMR (376 MHz, THF-d_8, 300 K): δ = −63.3 (s, CF_3) ppm.

$^{31}P\{^1H\}$ NMR (162 MHz, THF-d_8, 300 K): δ = 4.97 (s, $P(CH_3)_3$) ppm.

$^{31}P\{^1H\}$ NMR (162 MHz, 1,2-difluorobenzene-h_4/C_6D_6, 300 K): δ = 3.24 (s, $P(CH_3)_3$) ppm.

IR (KBr): ν_{CN} = 2063 cm^{-1}

The ^{13}C enriched isotopologue **[Co$_4$(^{13}CN)$_2$][BAr$^F_4$]$_2$** was synthesized as described above, using K^{13}CN as the CN$^-$ source. Selected data for **[Co$_4$(^{13}CN)$_2$][BAr$^F_4$]$_2$**: $^{13}C\{^1H\}$ NMR (126 MHz, THF-d_8, 300 K): δ = 176.4 (d, $^2J_{PC}$ = 15.1 Hz, C≡N) ppm.

NMR Spectra

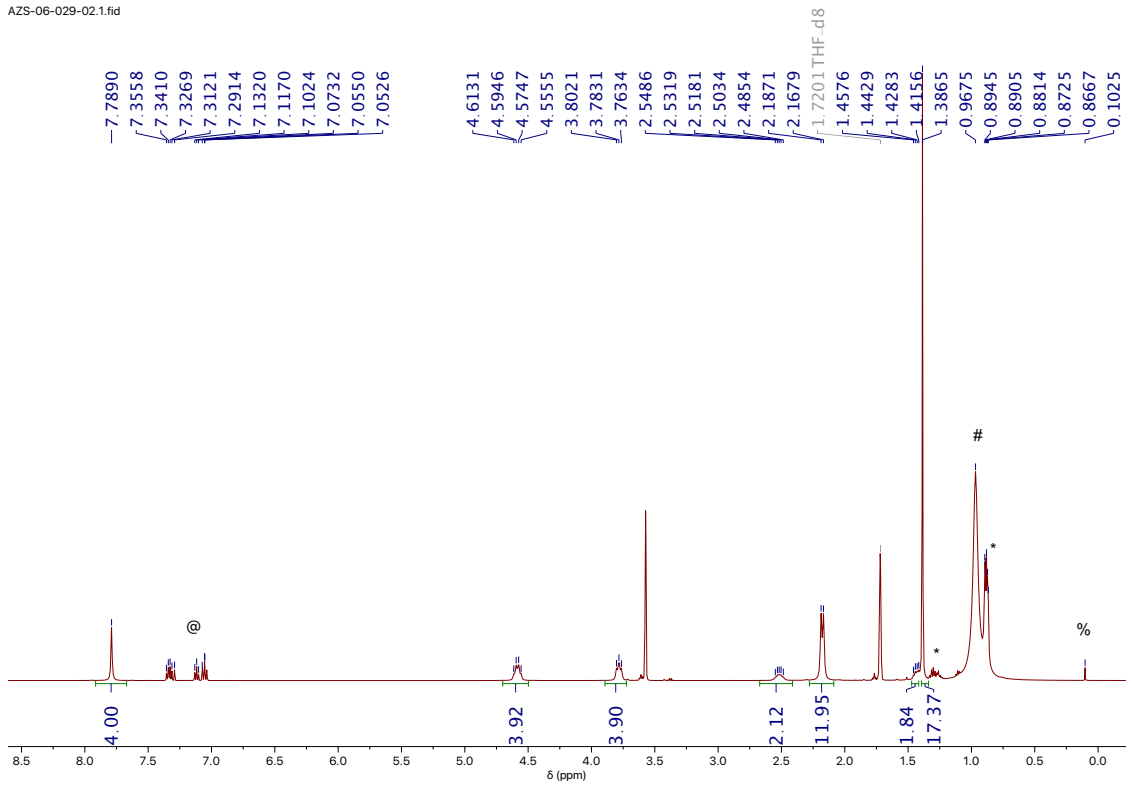

Figure S1: ^{1}H NMR spectrum of **[Co$_2$CN]$^+$** in THF-d_8 at 300 K. @ denotes co-crystallized fluorobenzene, * denotes co-crystallized pentane (overlapping with coordinated PMe$_3$). # denotes added free PMe$_3$, added to prevent dimerization. % denotes grease.

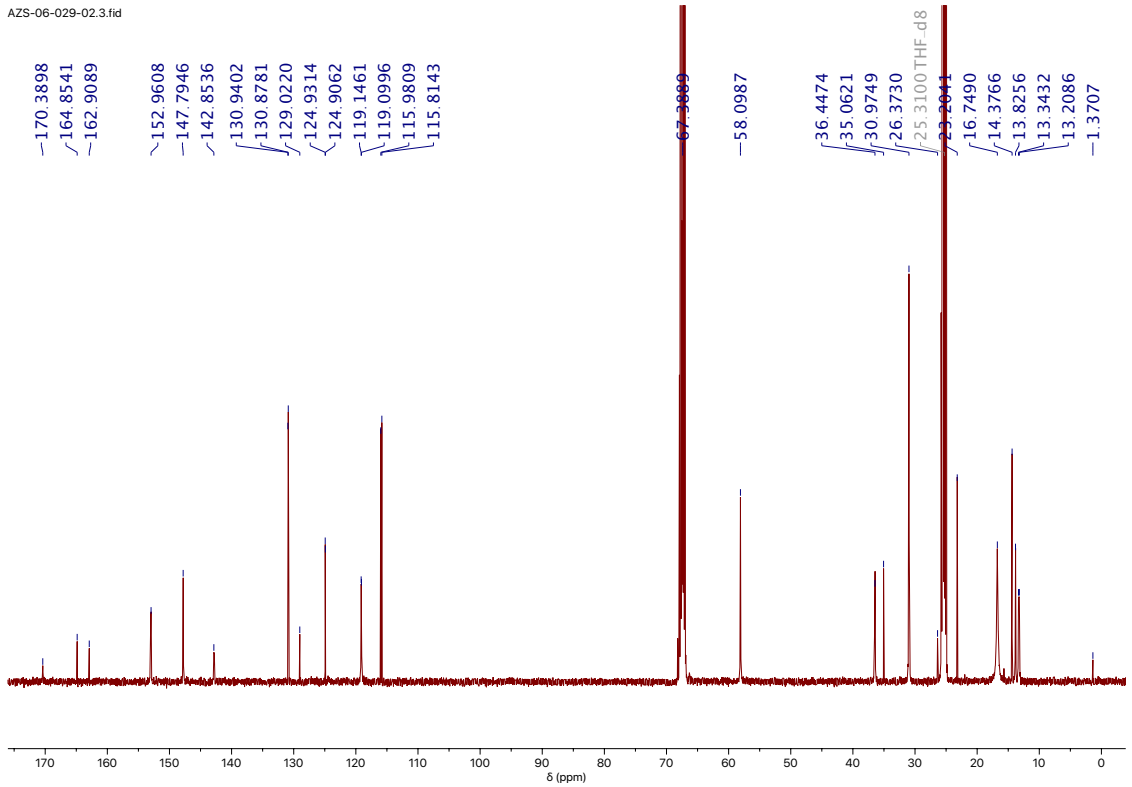

Figure S2: ^{13}C{^{1}H} NMR spectrum of **[Co$_2$CN]$^+$** in THF-d_8 with added PMe$_3$ at 300 K.

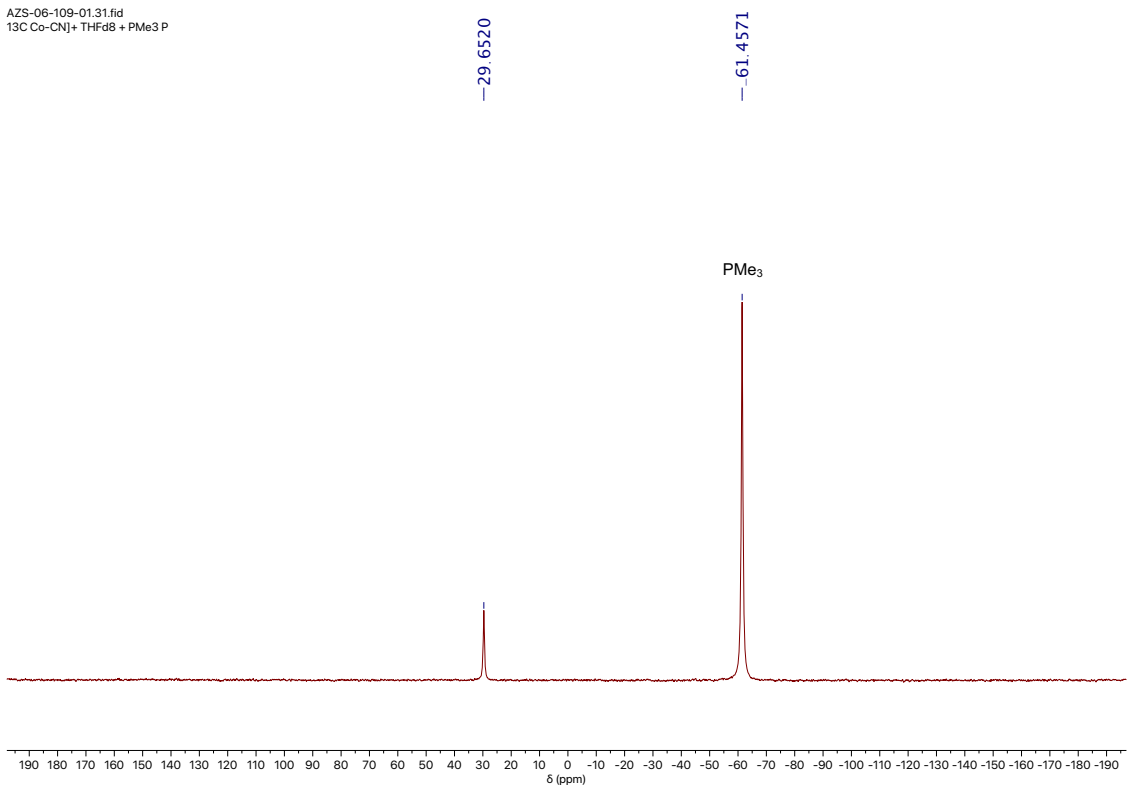

Figure S3: $^{31}P\{^{1}H\}$ NMR spectrum of **[Co₂CN]**$^{+}$ in THF-d_8 with added PMe_3 at 300 K .

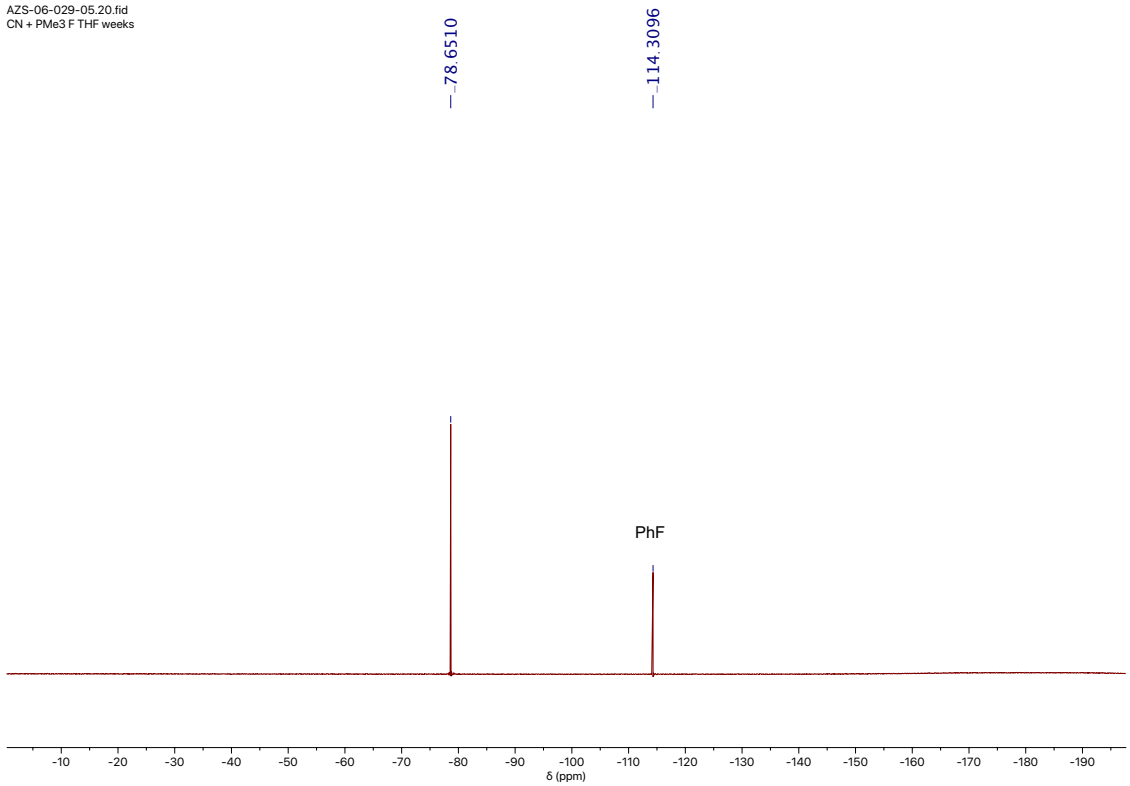

Figure S4: $^{19}F\{^{1}H\}$ NMR spectrum of **[Co₂CN]**$^{+}$ in THF-d_8 with added PMe_3 at 300 K.

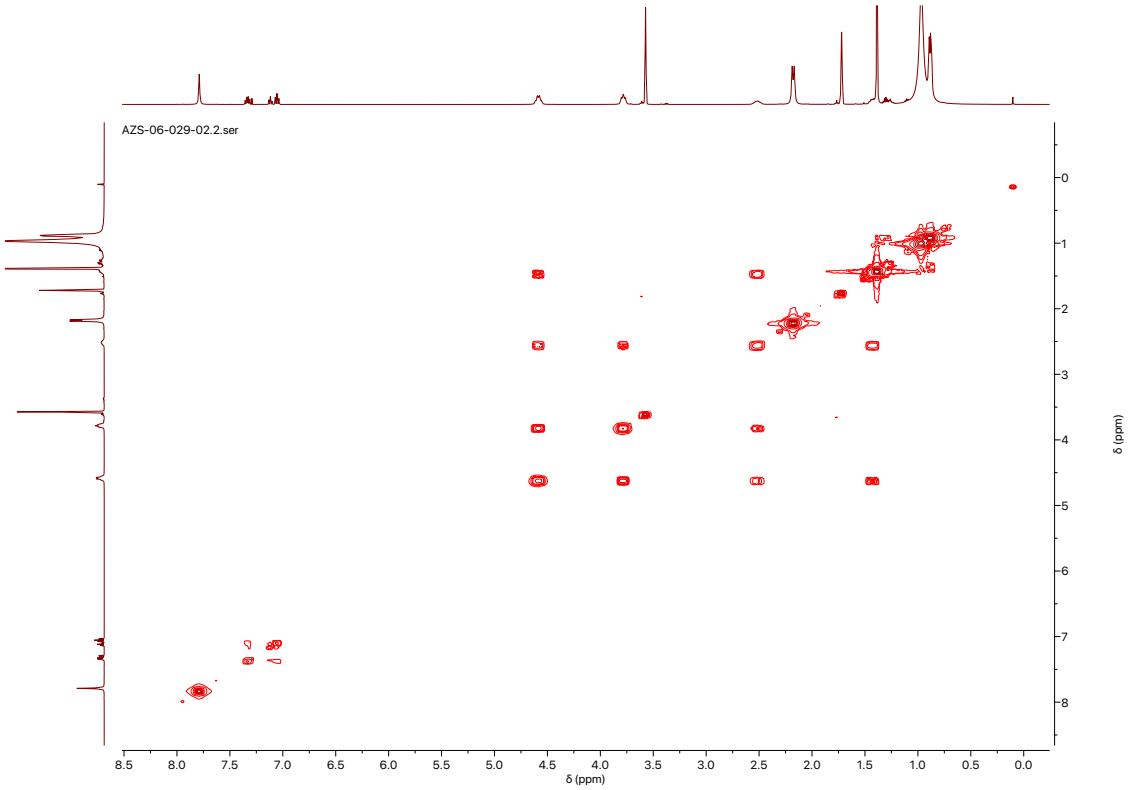

Figure S5: ^{1}H-^{1}H COSY spectrum of **[Co$_2$CN]$^+$** in THF-d_8 with added PMe$_3$ at 300 K.

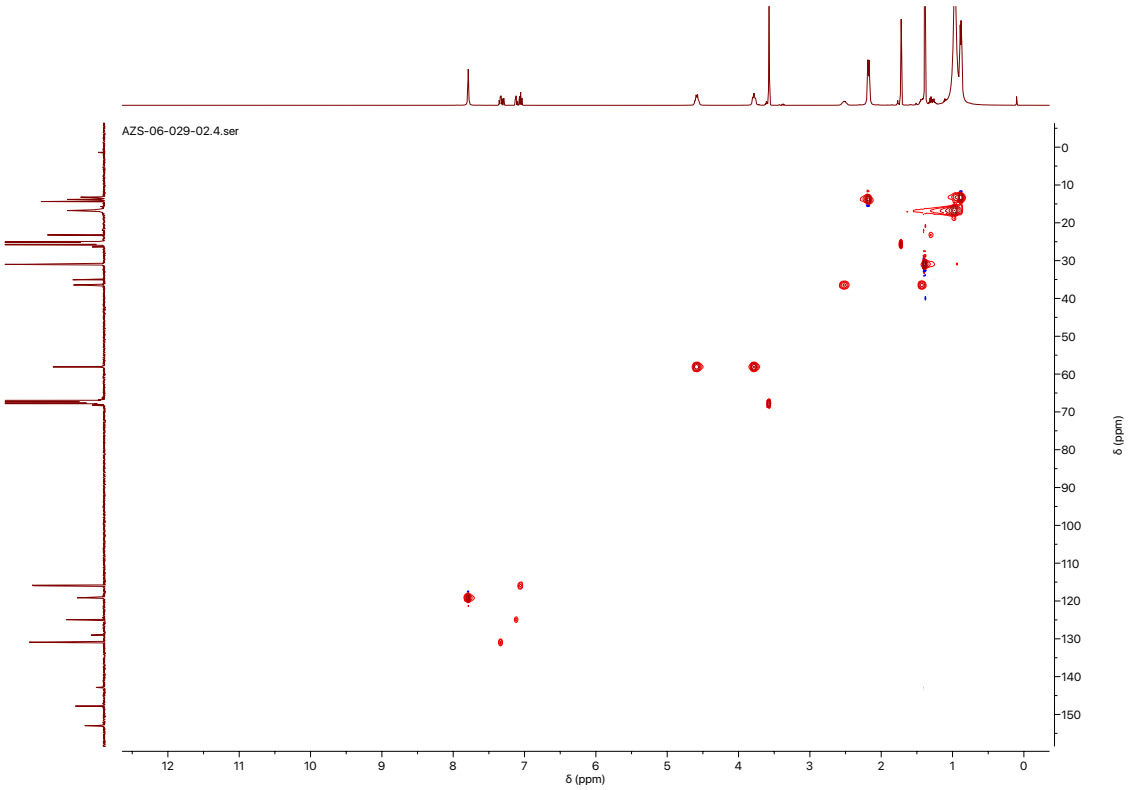

Figure S6: ^{1}H-^{13}C{^{1}H} HSQC spectrum of **[Co$_2$CN]$^+$** in THF-d_8 with added PMe$_3$ at 300 K.

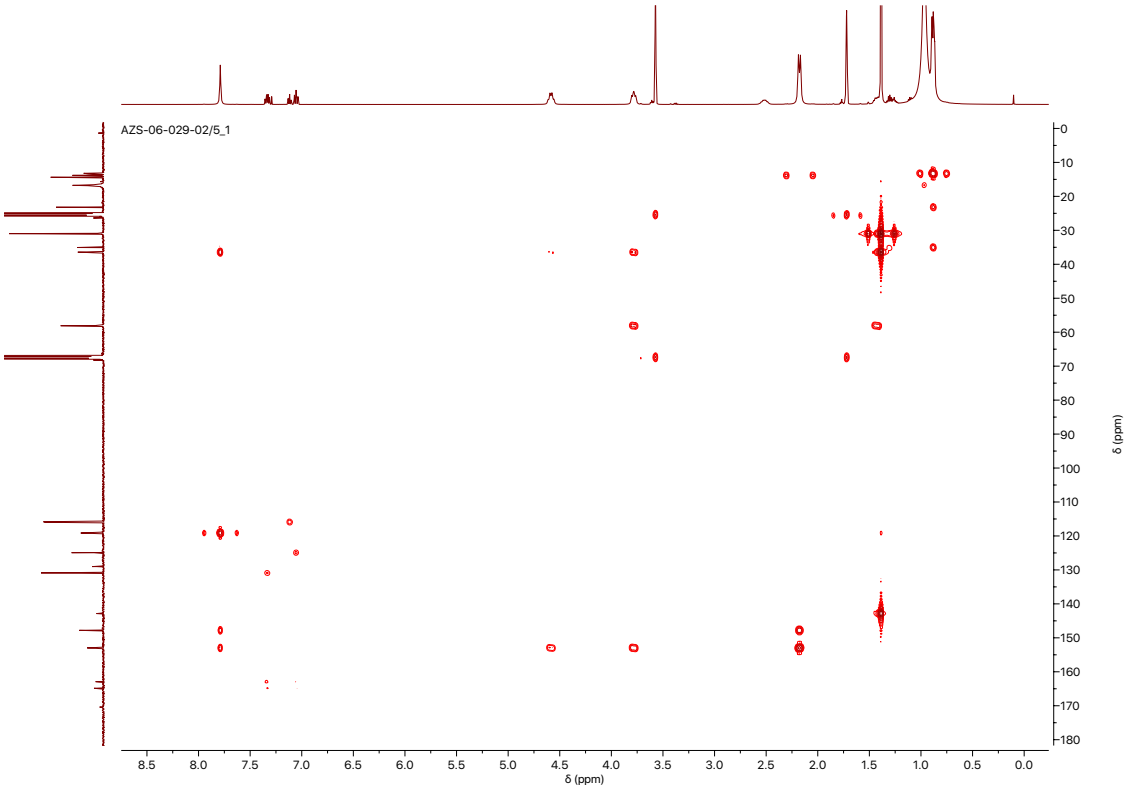

Figure S7: ^{1}H-^{13}C{^{1}H} HMBC spectrum of **[Co$_2$CN]$^+$** in THF-d_8 with added PMe$_3$ at 300 K.

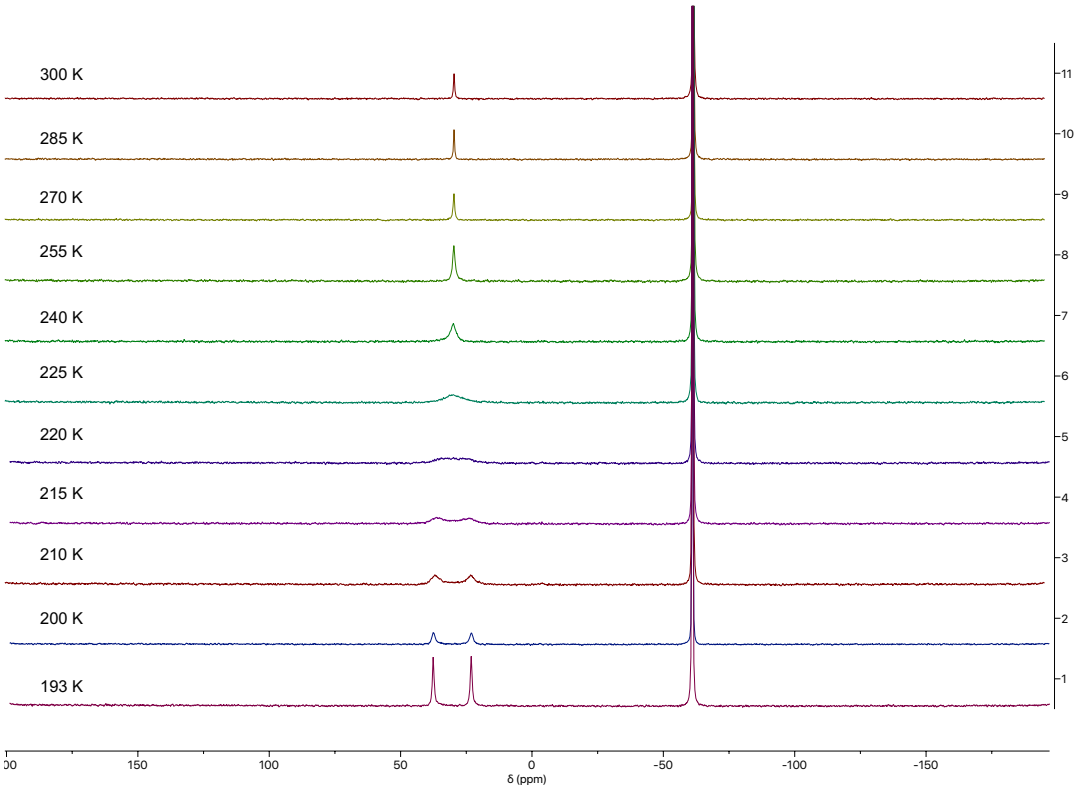

Figure S8: VT ^{31}P{^{1}H} NMR spectra of **[Co$_2$^{13}CN]$^+$** in THF-d_8 with added PMe$_3$.

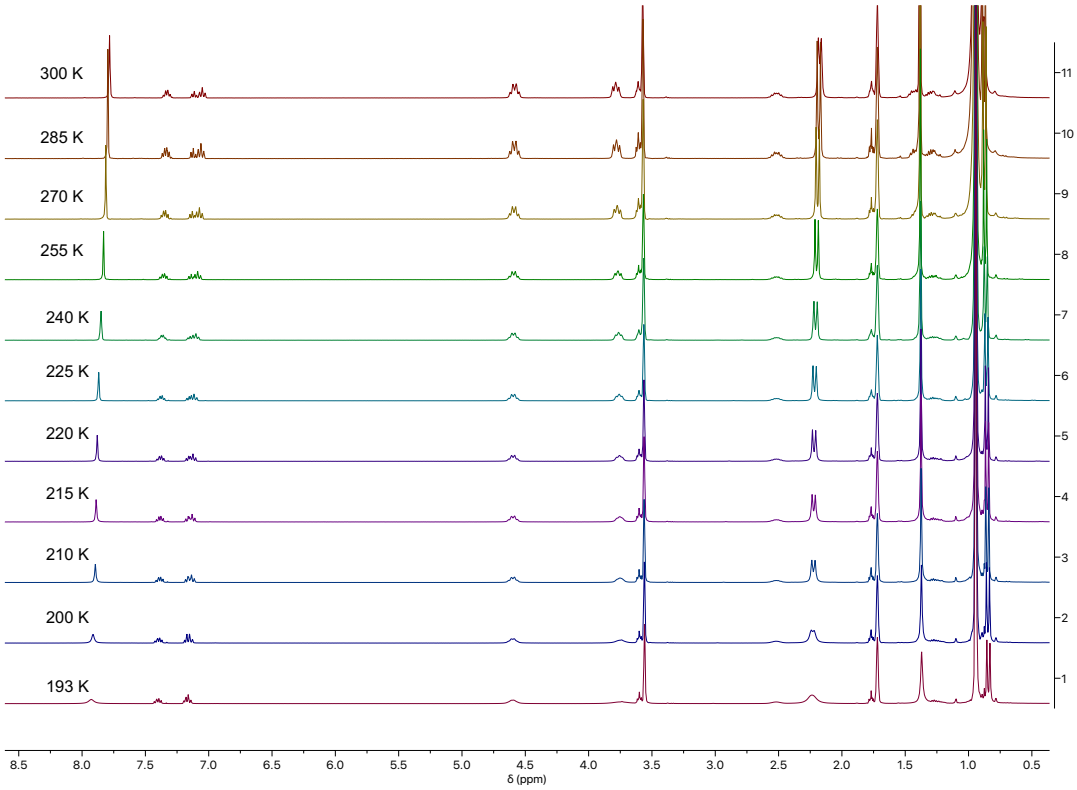

Figure S9: VT ^{1}H NMR spectra of **[Co$_2$^{13}CN]$^{+}$** in THF-d_8 with added PMe_3.

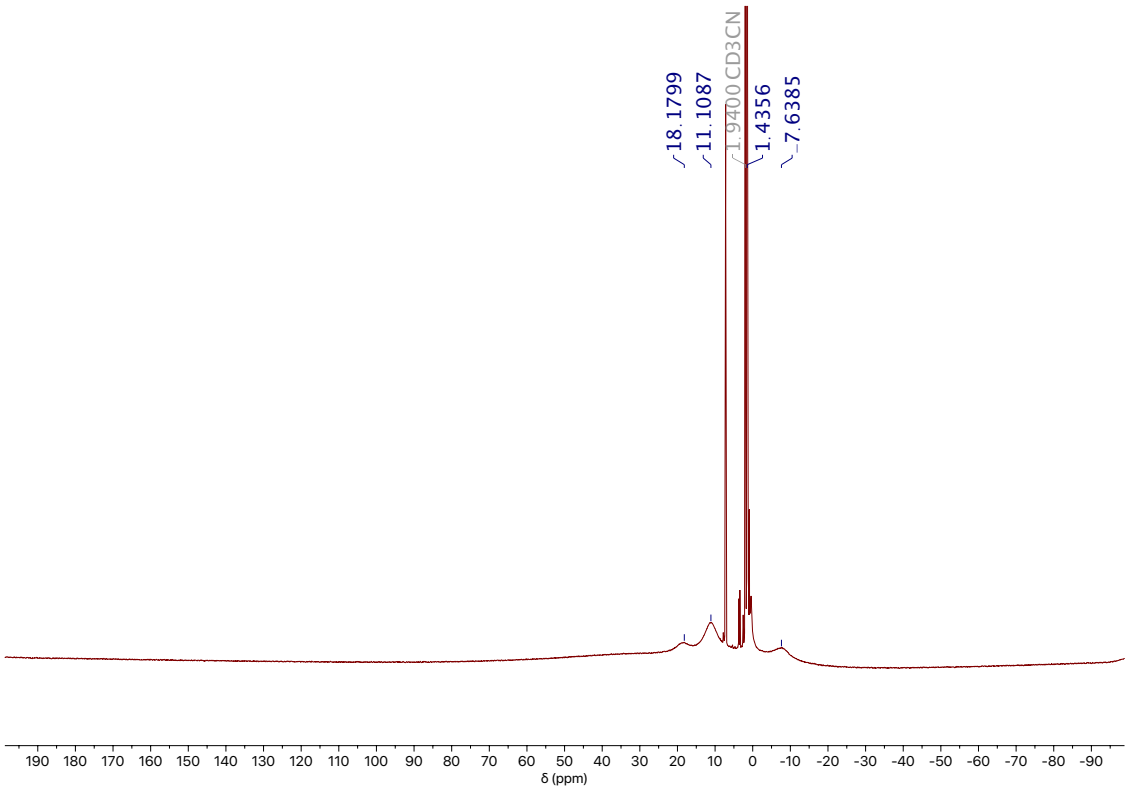

Figure S10: ^{1}H NMR spectrum of **[Co$_2$CN]$^{2+}$** in MeCN-d_3 at 300 K.

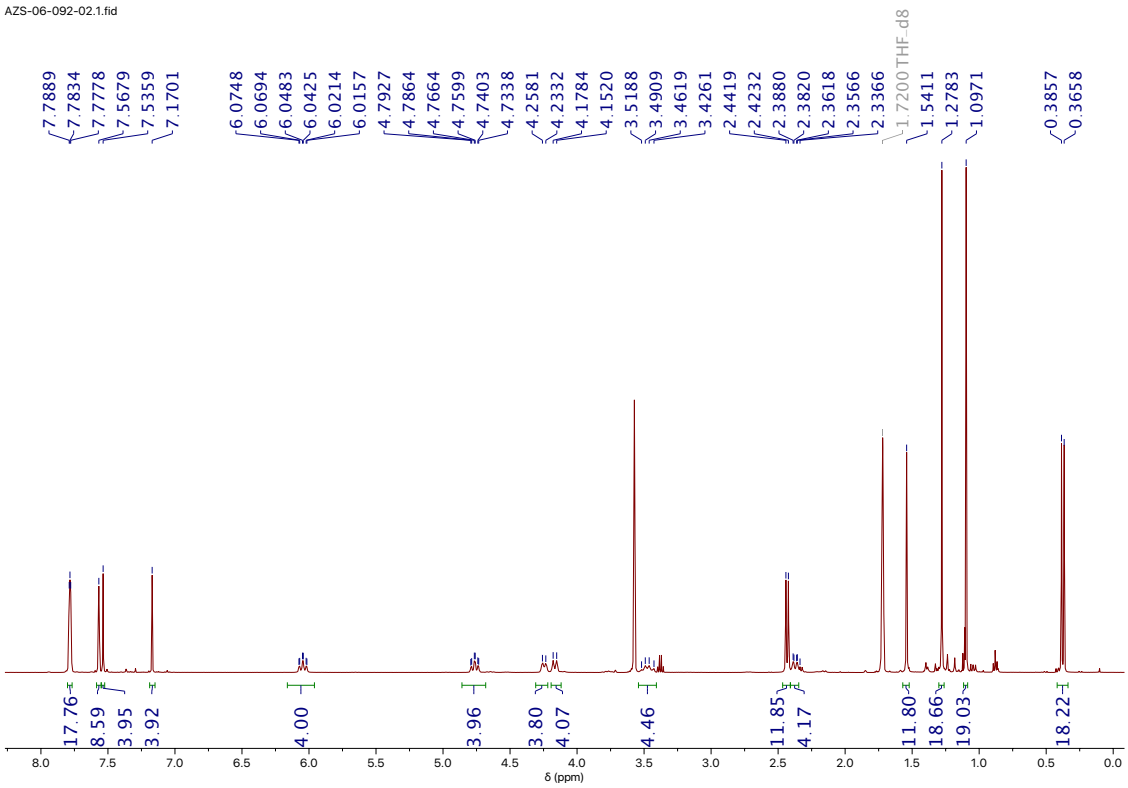

Figure S11: ^{1}H NMR spectrum of **[Co$_4$(CN)$_2$][BAr$^F_4$]$_2$** in THF-d_8 at 300 K.

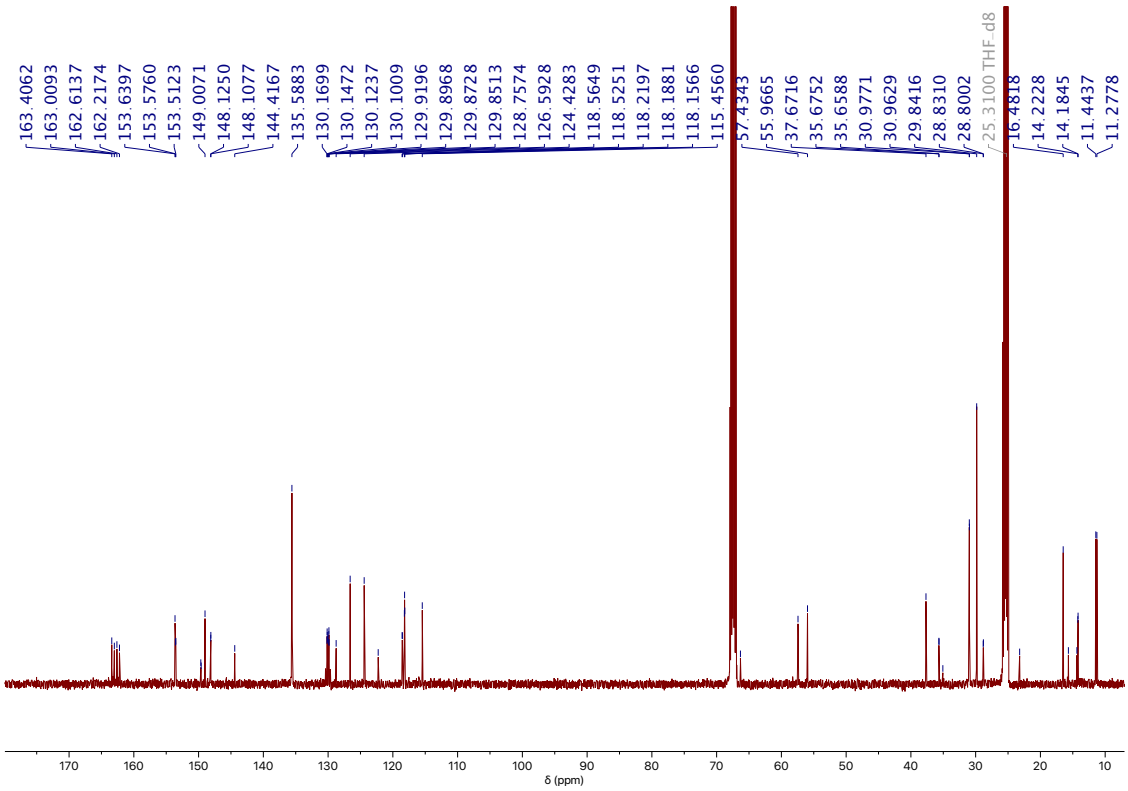

Figure S12: ^{13}C{^{1}H} NMR spectrum of **[Co$_4$(CN)$_2$][BAr$^F_4$]$_2$** in THF-d_8 at 300 K.

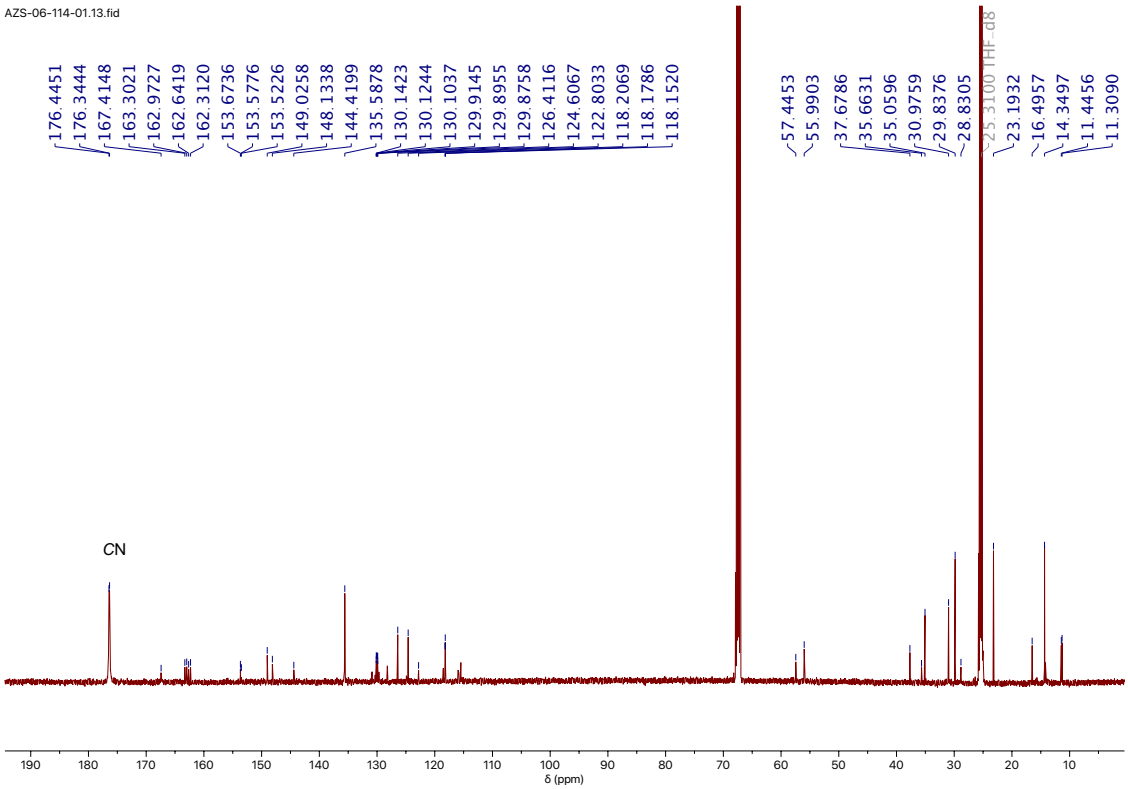

Figure S13: $^{13}C\{^{1}H\}$ NMR spectrum of **[Co$_4$(^{13}CN)$_2$][BAr$^F_4$]$_2$** in THF-d_8 at 300 K.

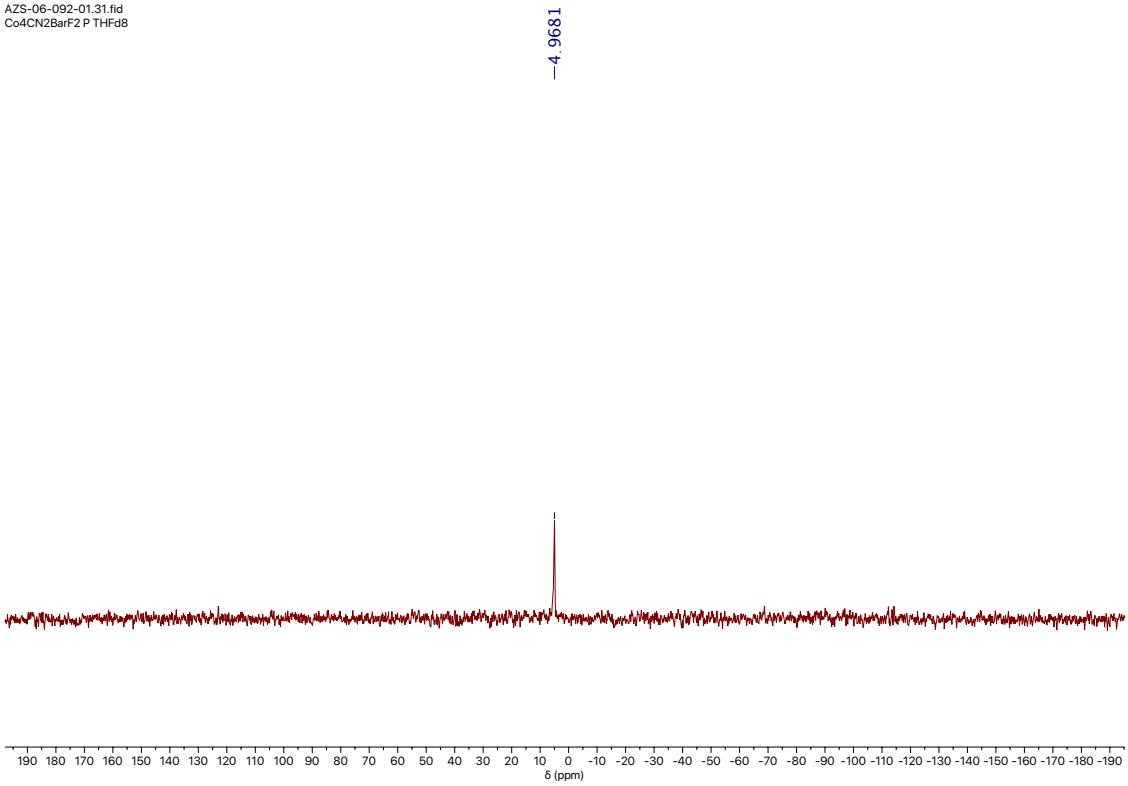

Figure S14: $^{31}P\{^{1}H\}$ NMR spectrum of **[Co$_4$(CN)$_2$][BAr$^F_4$]$_2$** in THF-d_8 at 300 K.

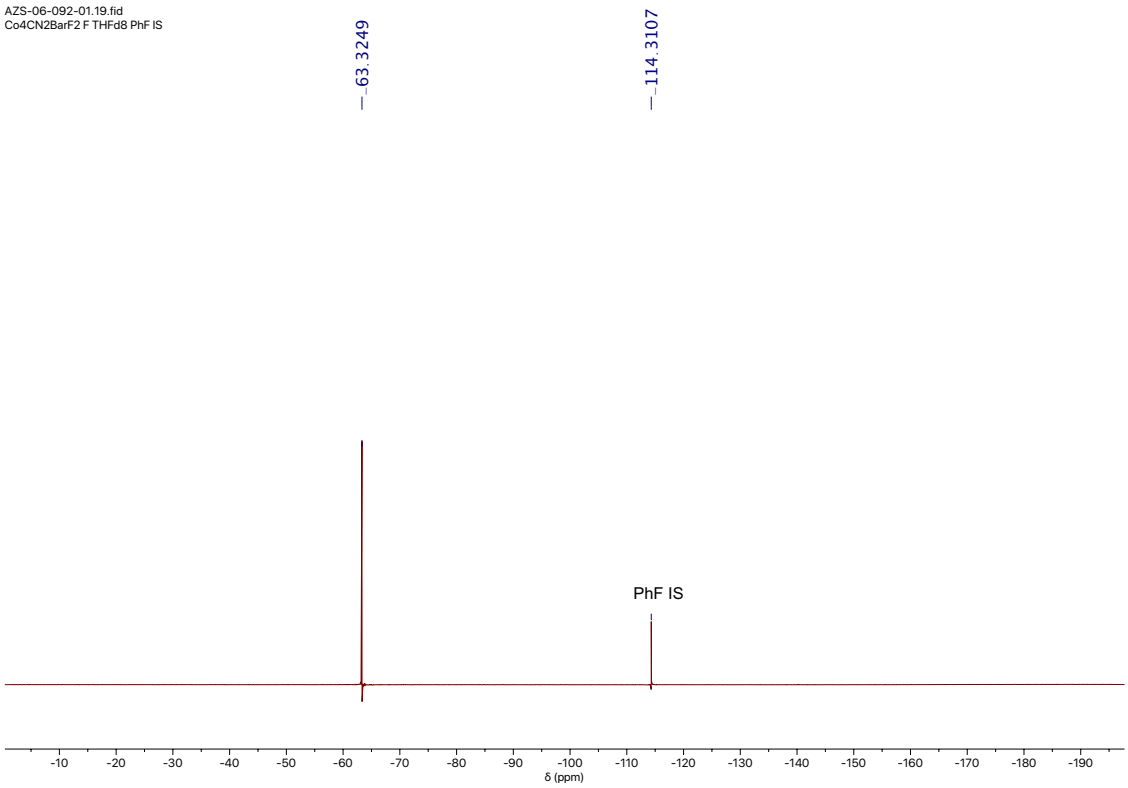

Figure S15: $^{19}F\{^{1}H\}$ NMR spectrum of **[Co$_4$(CN)$_2$][BAr^F$_4$]$_2$** in THF-d_8 with PhF internal standard at 300 K.

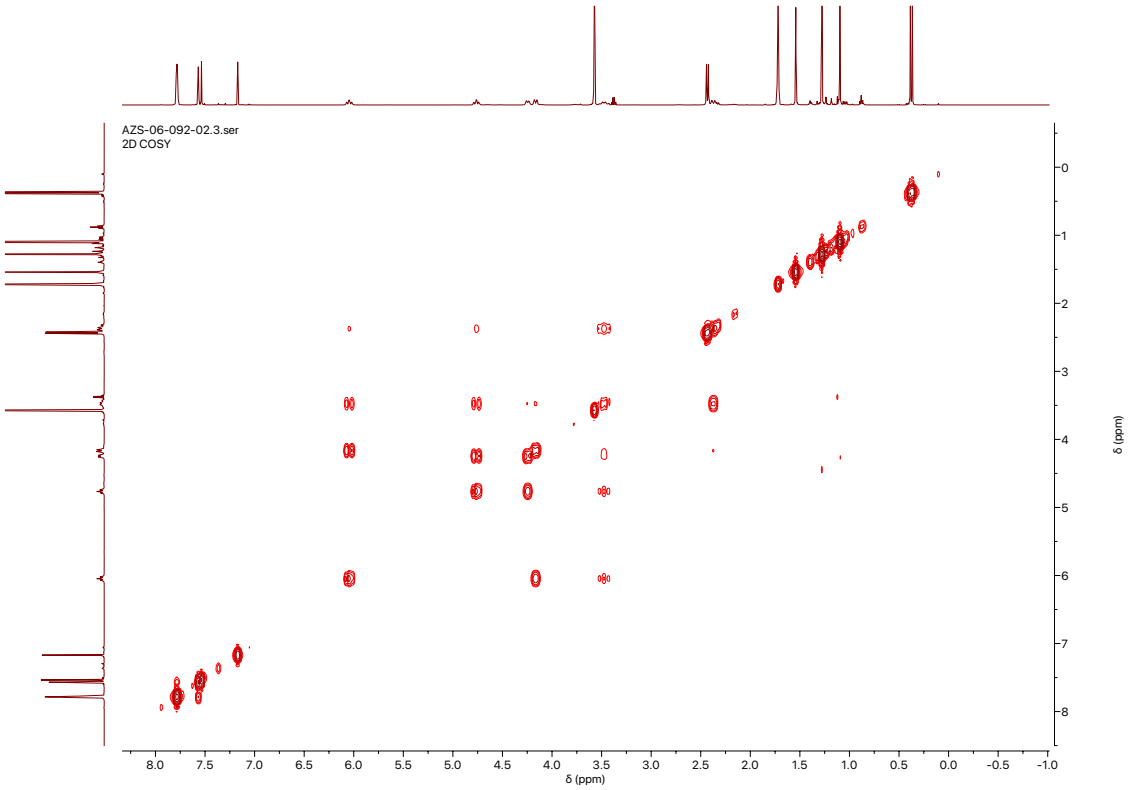

Figure S16: ^{1}H-^{1}H COSY spectrum of **[Co$_4$(CN)$_2$][BAr^F$_4$]$_2$** in THF-d_8 at 300 K.

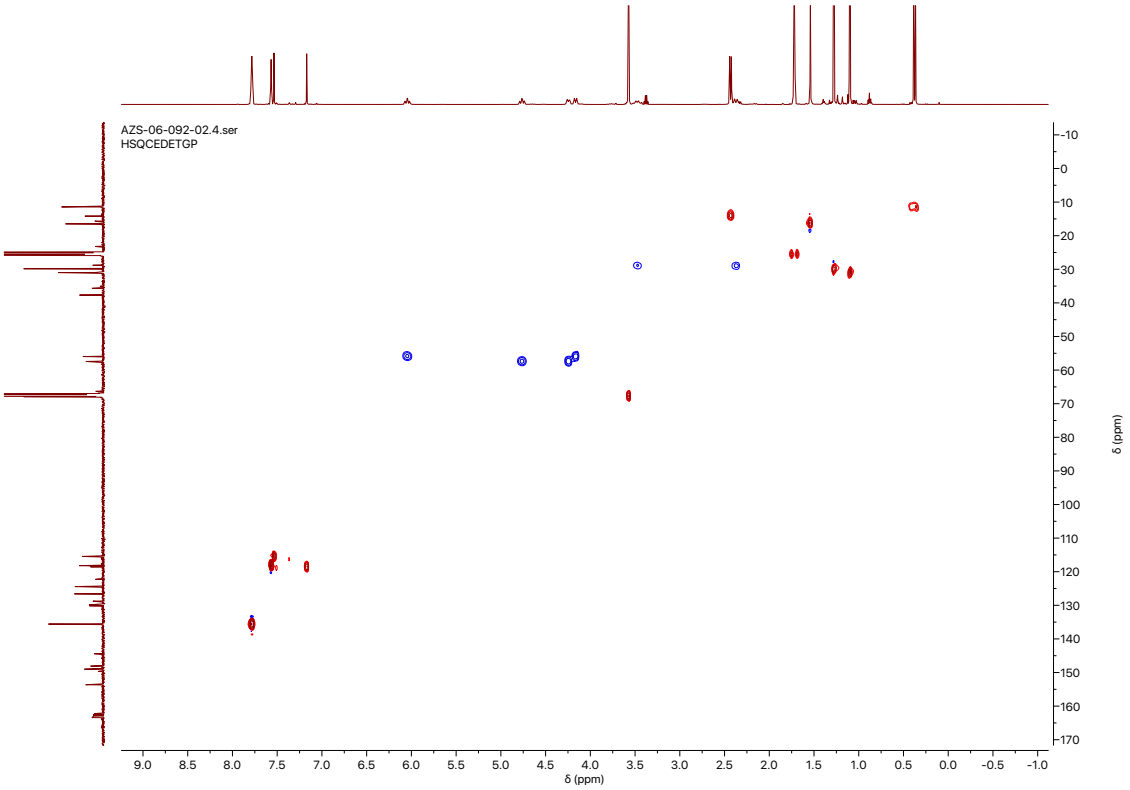

Figure S17: ^{1}H-^{13}C{^{1}H} HSQC spectrum of **[Co$_4$(CN)$_2$][BAr^F$_4$]$_2$** in THF-d_8 at 300 K.

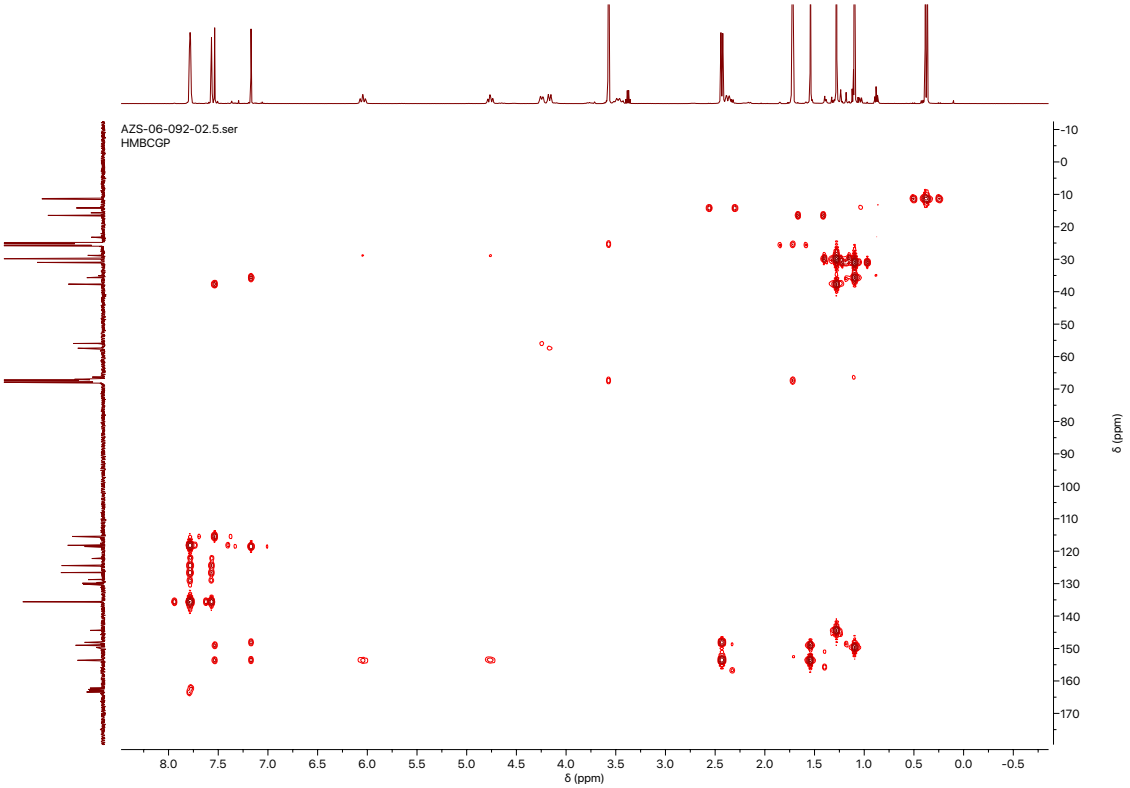

Figure S18: ^{1}H-^{13}C{^{1}H} HMBC spectrum of **[Co$_4$(CN)$_2$][BAr^F$_4$]$_2$** in THF-d_8 at 300 K.

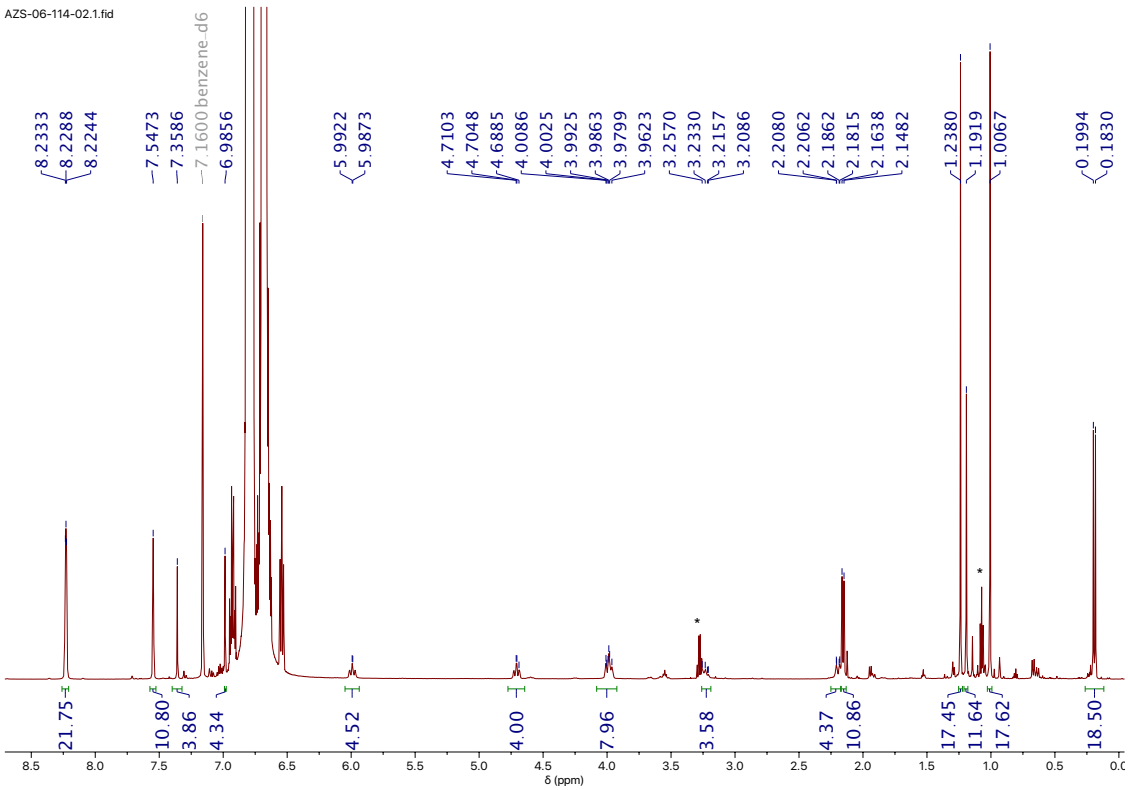

Figure S19: ^{1}H NMR spectrum of **[Co$_4$(CN)$_2$][BAr$^F_4$]$_2$** in 1,2-difluorobenzene-*h*$_4$/C$_6$D$_6$ at 300 K.

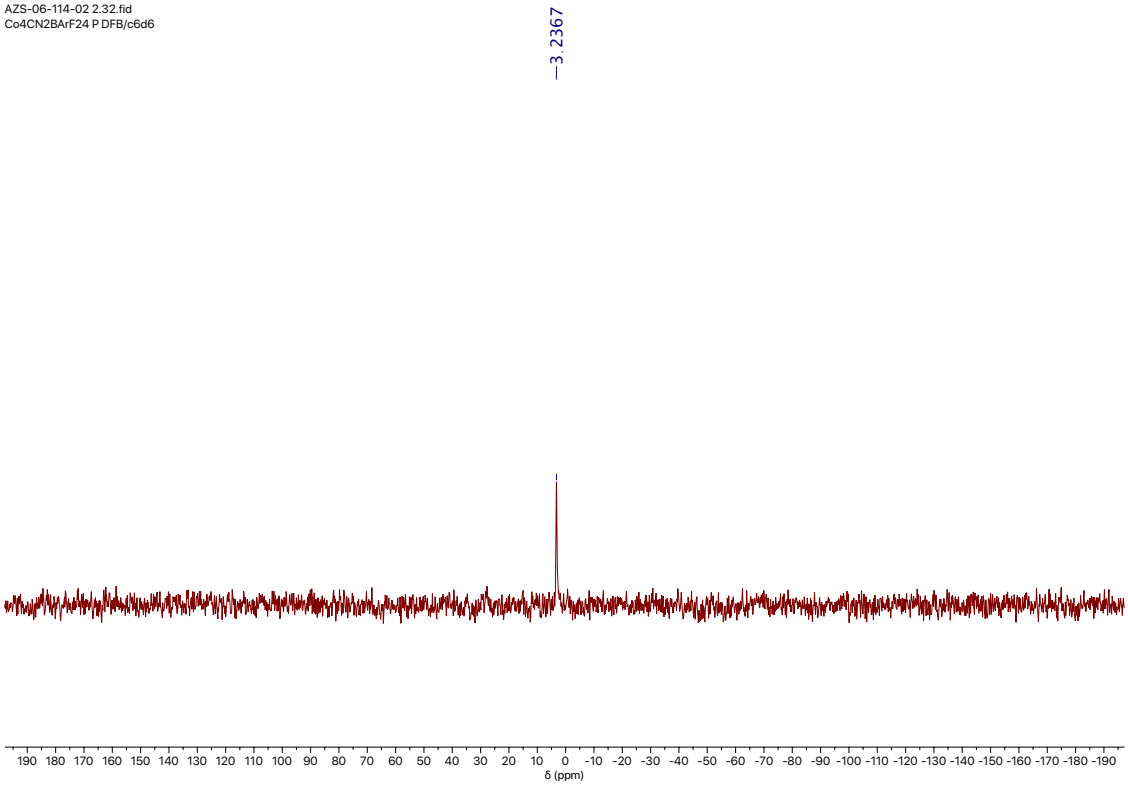

Figure S20: ^{31}P{^{1}H} NMR spectrum of **[Co$_4$(CN)$_2$][BAr$^F_4$]$_2$** in 1,2-difluorobenzene-*h*$_4$/C$_6$D$_6$.

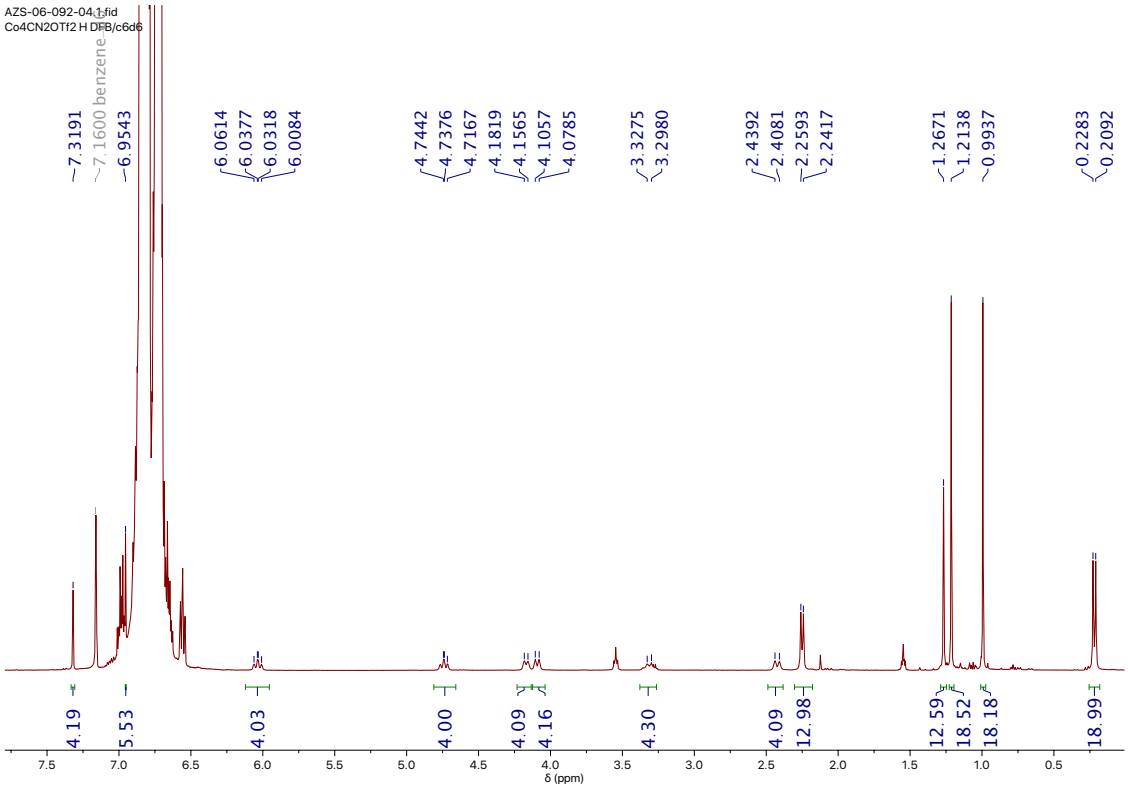

Figure S21: ^{1}H NMR spectrum of **[Co$_4$(CN)$_2$][OTf]$_2$** in 1,2-difluorobenzene-h_4/C_6D_6.

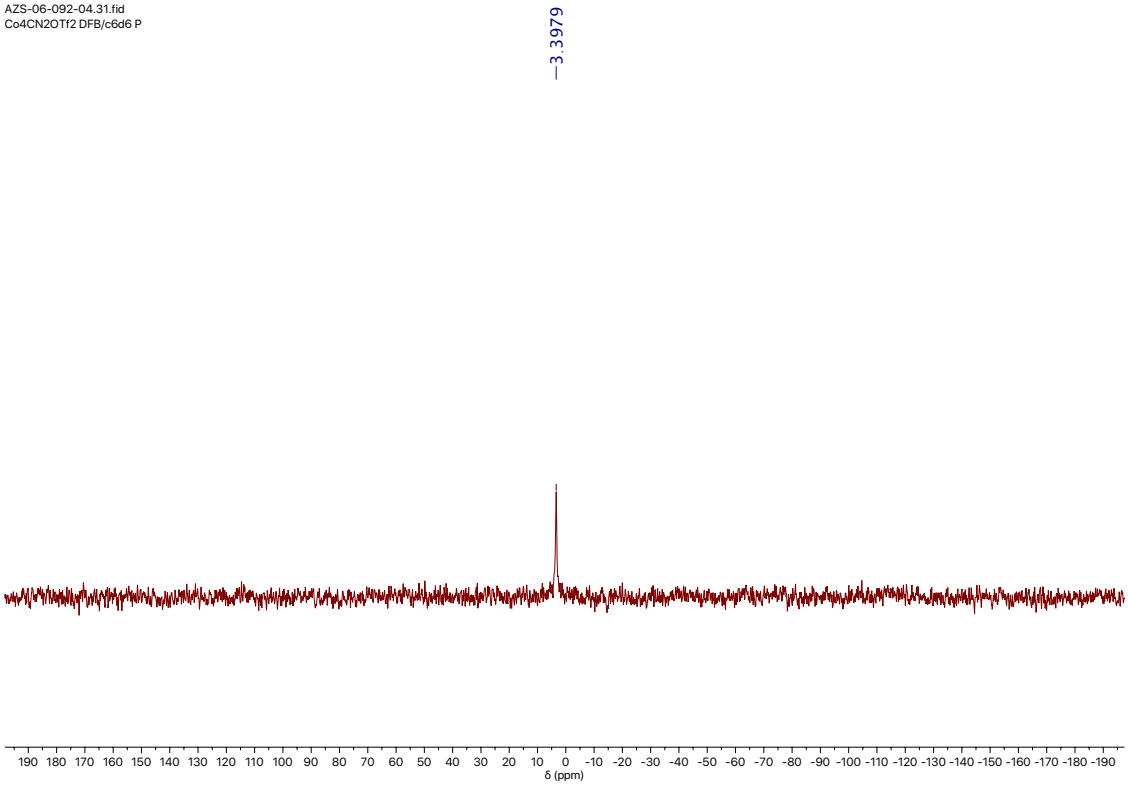

Figure S22: ^{31}P{^{1}H} NMR spectrum of **[Co$_4$(CN)$_2$][OTf]$_2$** in 1,2-difluorobenzene-h_4/C_6D_6 at 300 K.

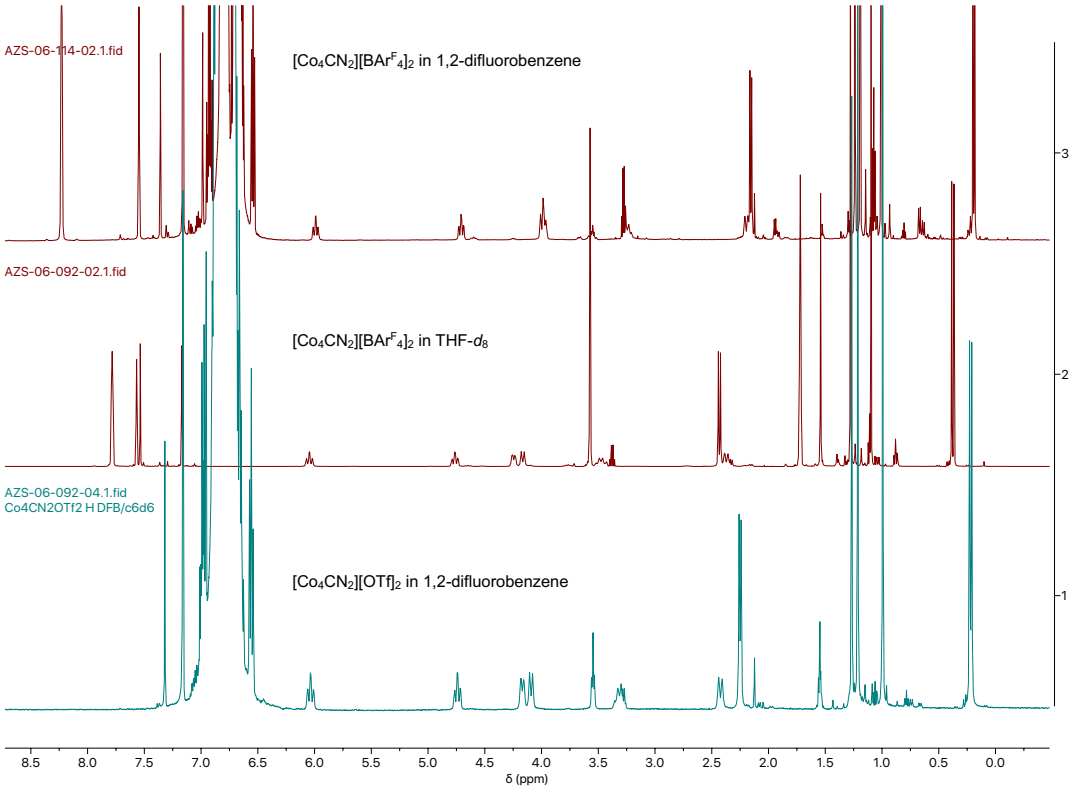

Figure S23: Stacked ^{1}H NMR spectra of **[Co$_4$(CN)$_2$][OTf]$_2$** and **[Co$_4$(CN)$_2$][BAr^F$_4$]$_2$** in 1,2-difluorobenzene-h_4/C_6D_6, as well as **[Co$_4$(CN)$_2$][BAr^F$_4$]$_2$** in THF-d_8 at 300 K.

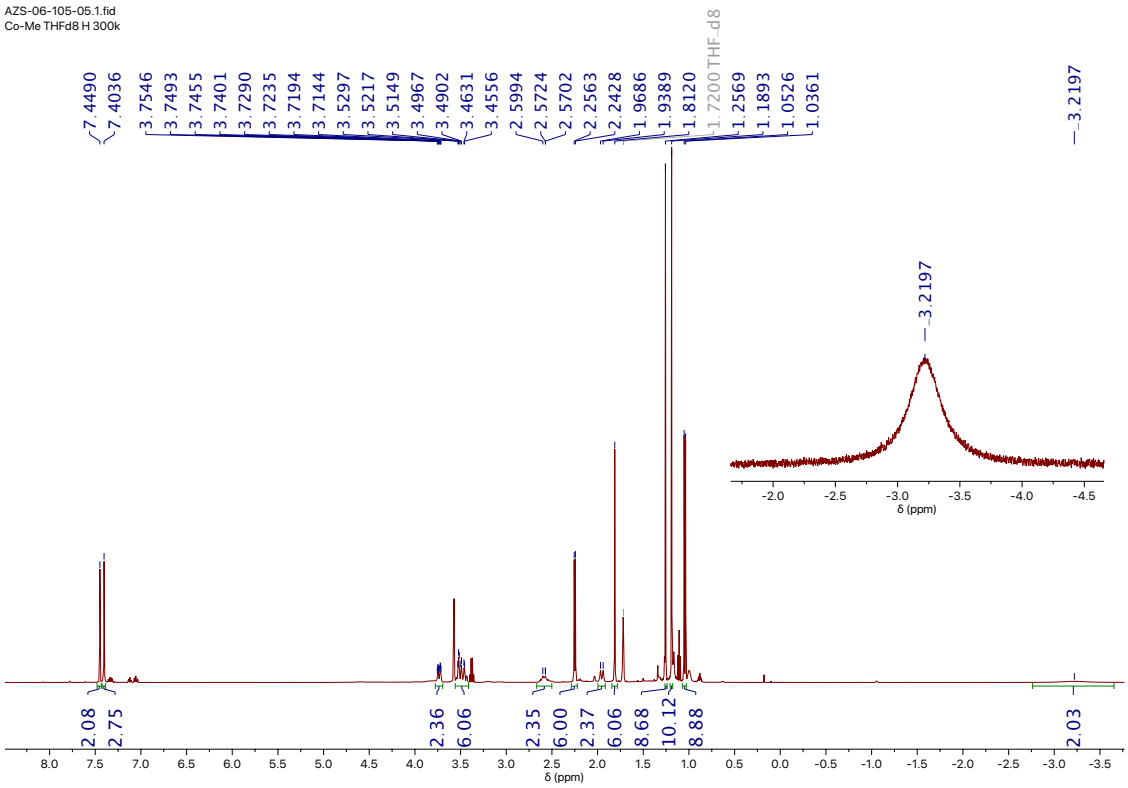

Figure S24: ^{1}H NMR spectrum of **[Co$_2$CH$_3$]$^+$** in THF-d_8 at 300 K.

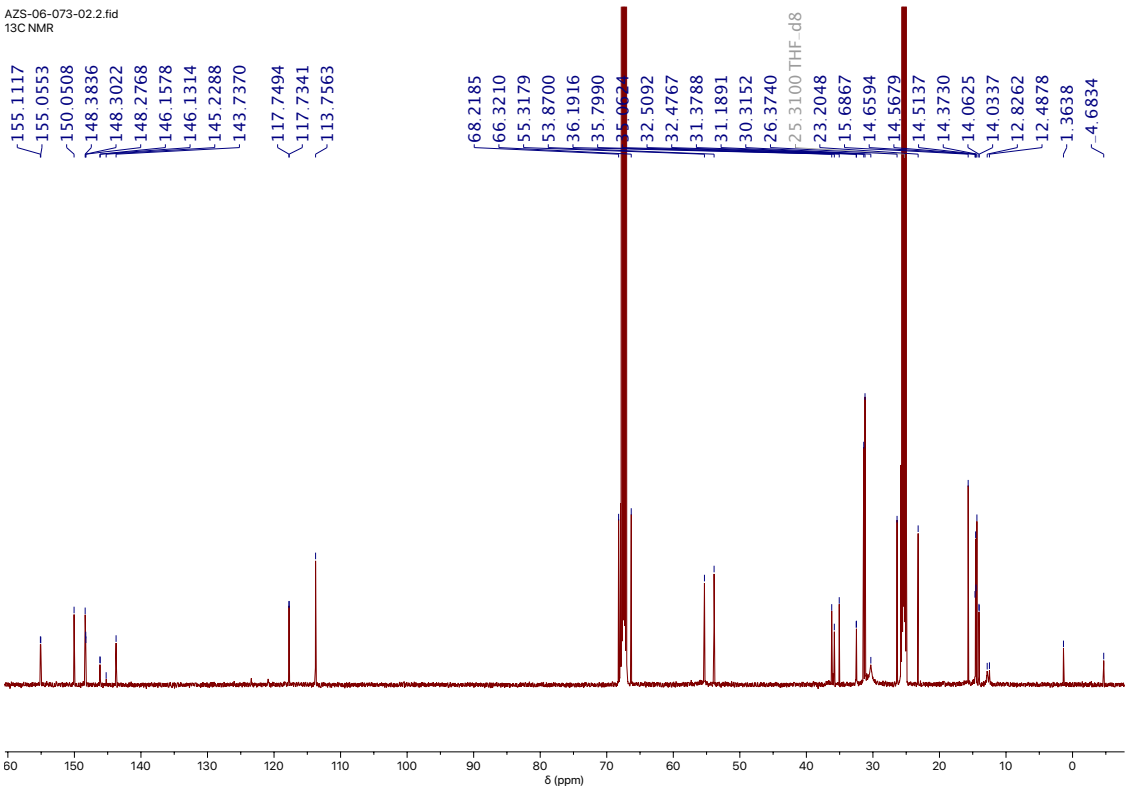

Figure S25: $^{13}C\{^{1}H\}$ NMR spectrum of **[Co_2CH_3]**$^+$ in THF-d_8 at 300 K.

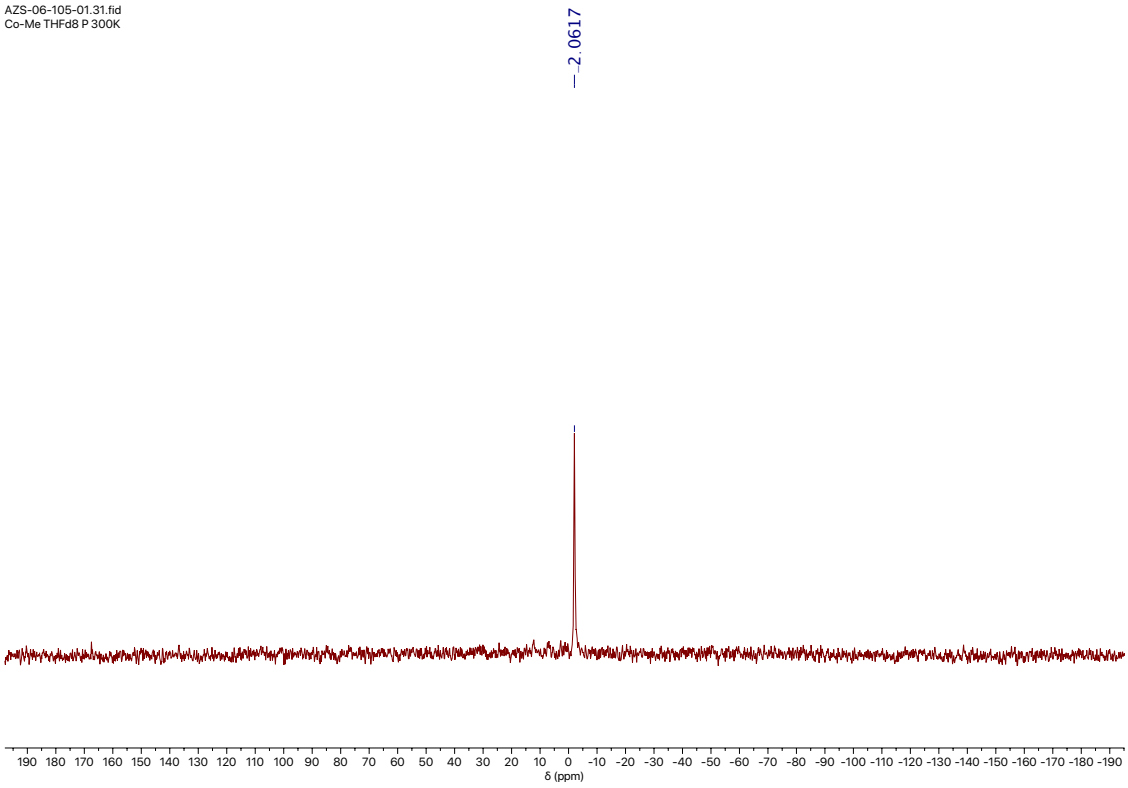

Figure S26: $^{31}P\{^{1}H\}$ NMR spectrum of **[Co_2CH_3]**$^+$ in THF-d_8 at 300 K.

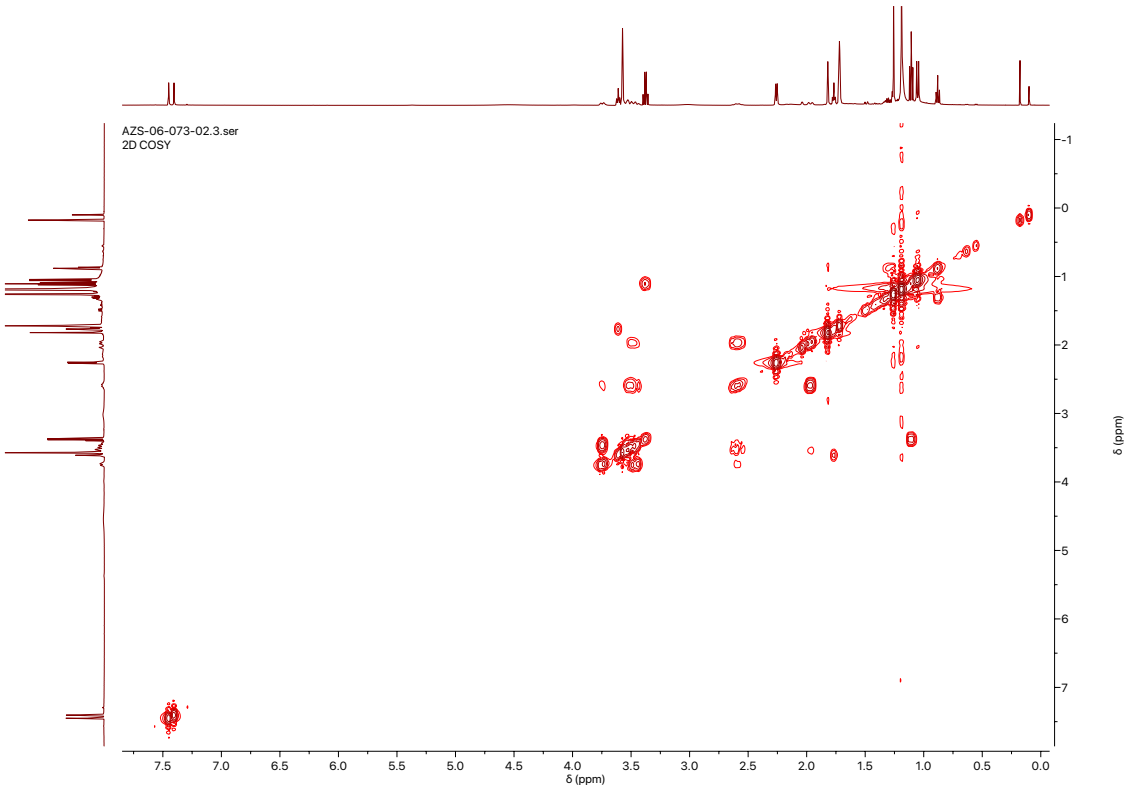

Figure S27: ^{1}H-^{1}H COSY spectrum of **[Co$_2$CH$_3$]$^+$** in THF-d_8 at 300 K.

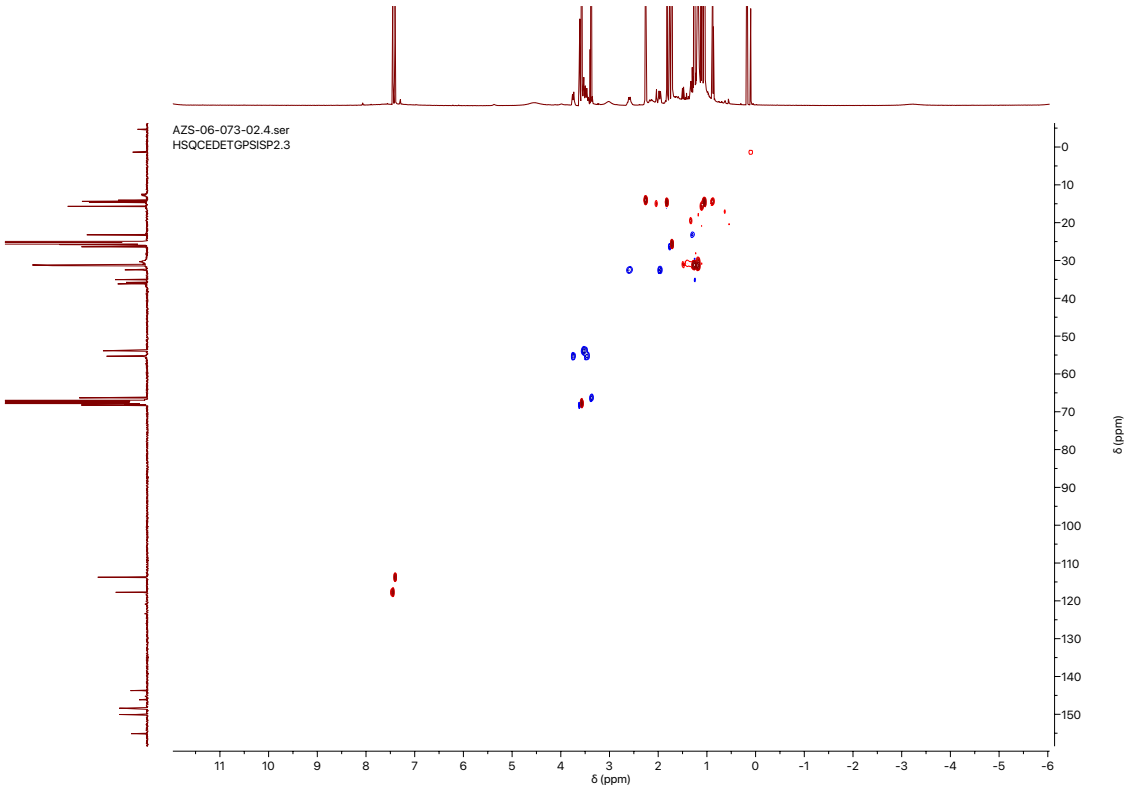

Figure S28: ^{1}H-^{13}C{^{1}H} HSQC spectrum of **[Co$_2$CH$_3$]$^+$** in THF-d_8 at 300 K.

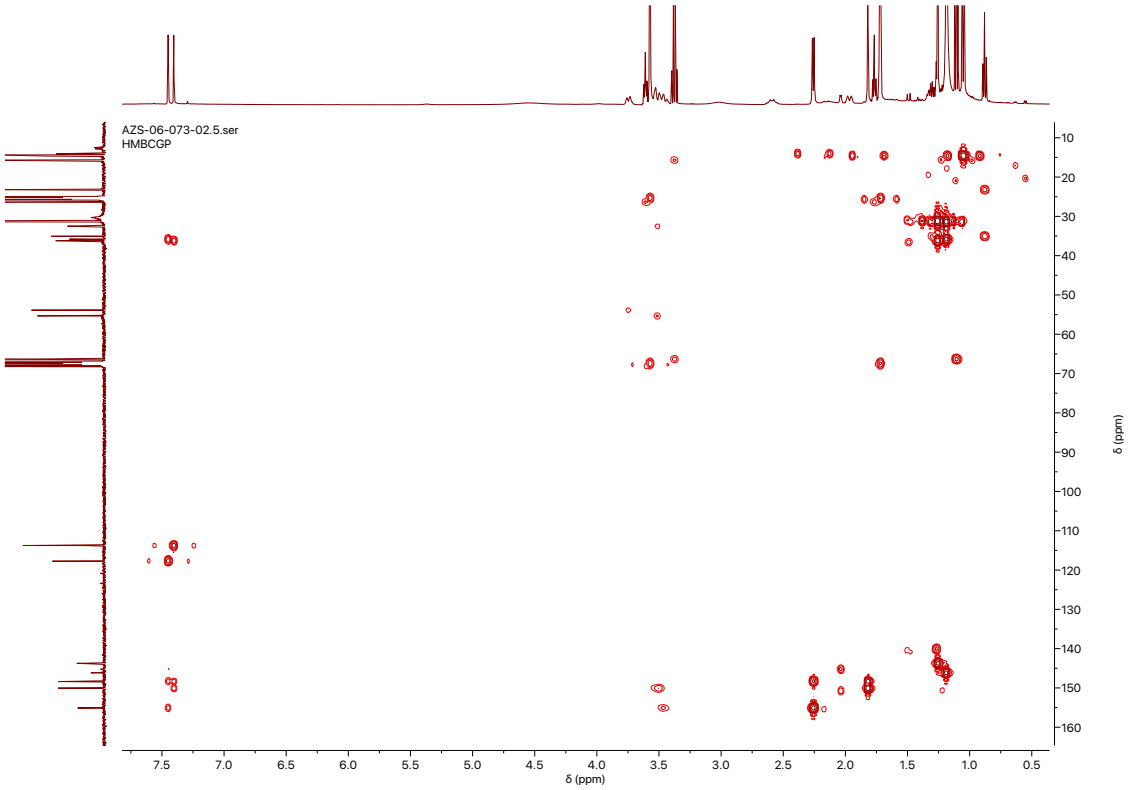

Figure S29: ^{1}H-^{13}C{^{1}H} HMBC spectrum of **[Co$_2$CH$_3$]**$^+$ in THF-d_8 at 300 K.

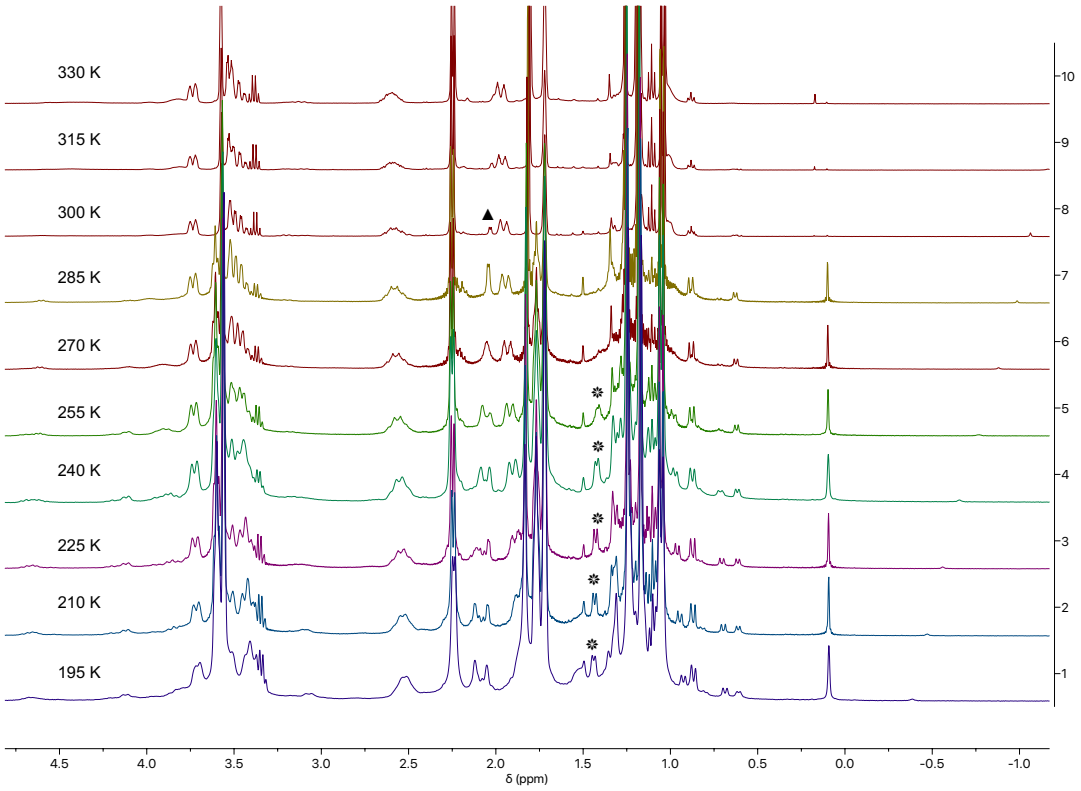

Figure S30: VT ^{1}H NMR spectra of **[Co$_2$CH$_3$]**$^+$ in THF-d_8. ✻ denotes proposed bridging CH_2H moiety. Note two separate samples were used for high temperature and low temperature data collection, accounting for the difference in residual solvents. ▲ denotes a signal from a small amount of a known, Co-containing diamagnetic impurity.

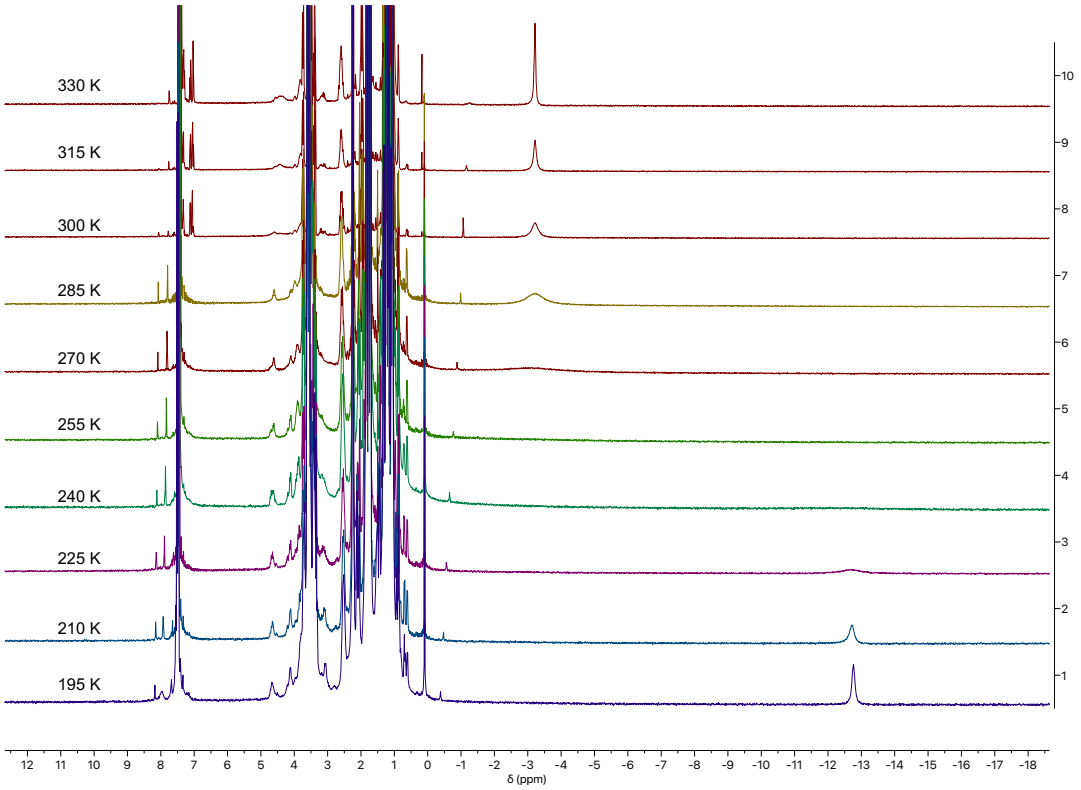

Figure S31: VT ^{1}H NMR spectra of **[Co$_2$CH$_3$]$^+$** in THF-d_8 showing upfield region.

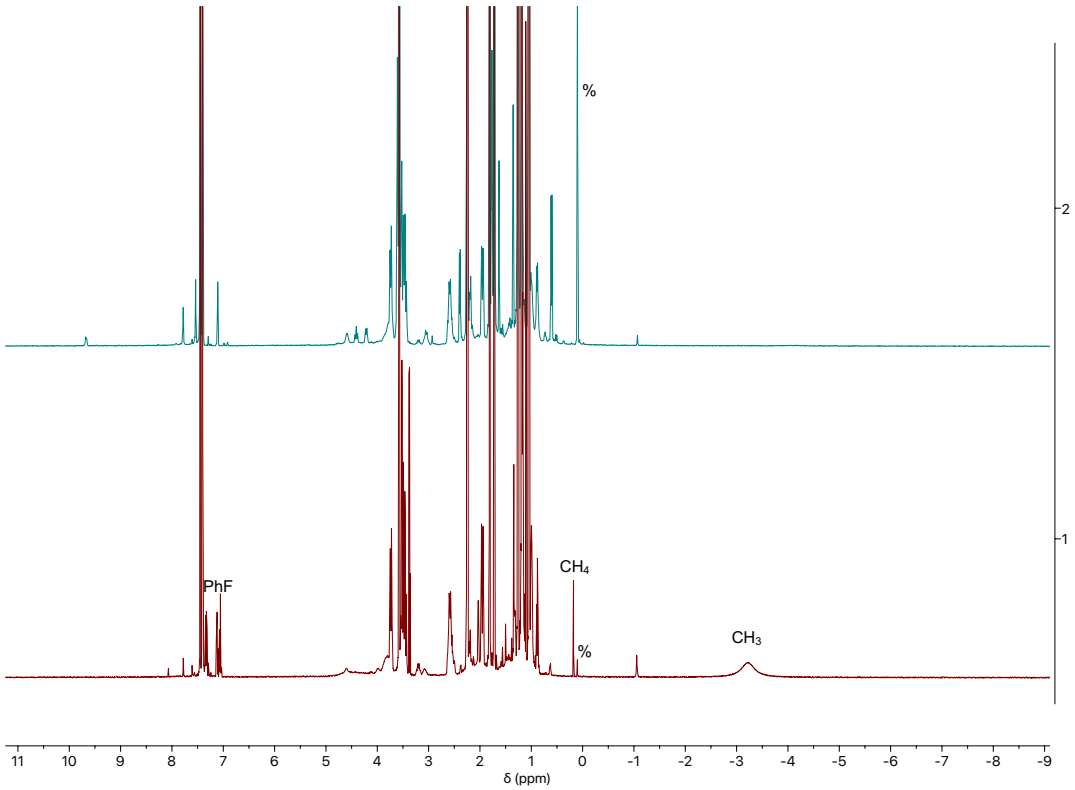

Figure S32: Top: ^{1}H NMR spectrum of **[Co$_2$CD$_3$]$^+$** in THF-d_8 at 300 K made from CD_3CN. Bottom: ^{1}H NMR spectrum of **[Co$_2$CH$_3$]$^+$** in THF-d_8 at 300 K made from CH_3CN. % denotes grease.

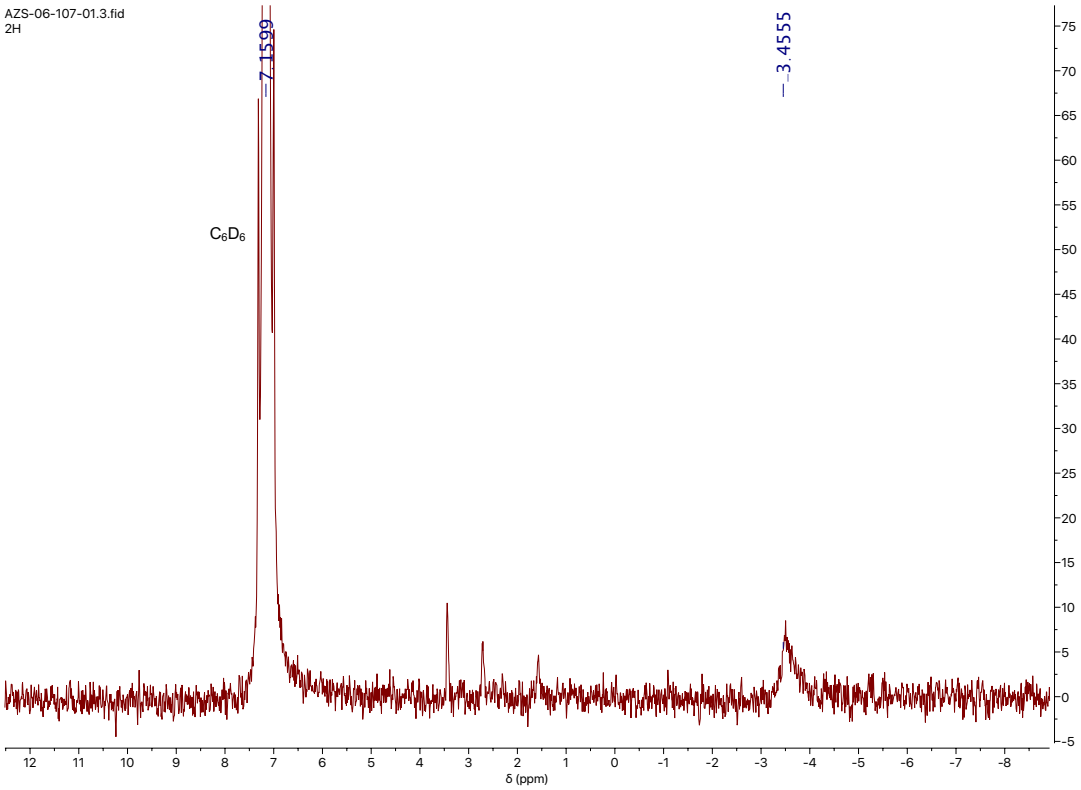

Figure S33: ^{2}H NMR spectrum of **[Co$_2$CD$_3$]$^+$** in THF-h_8 with one drop of C_6D_6 at 300 K.

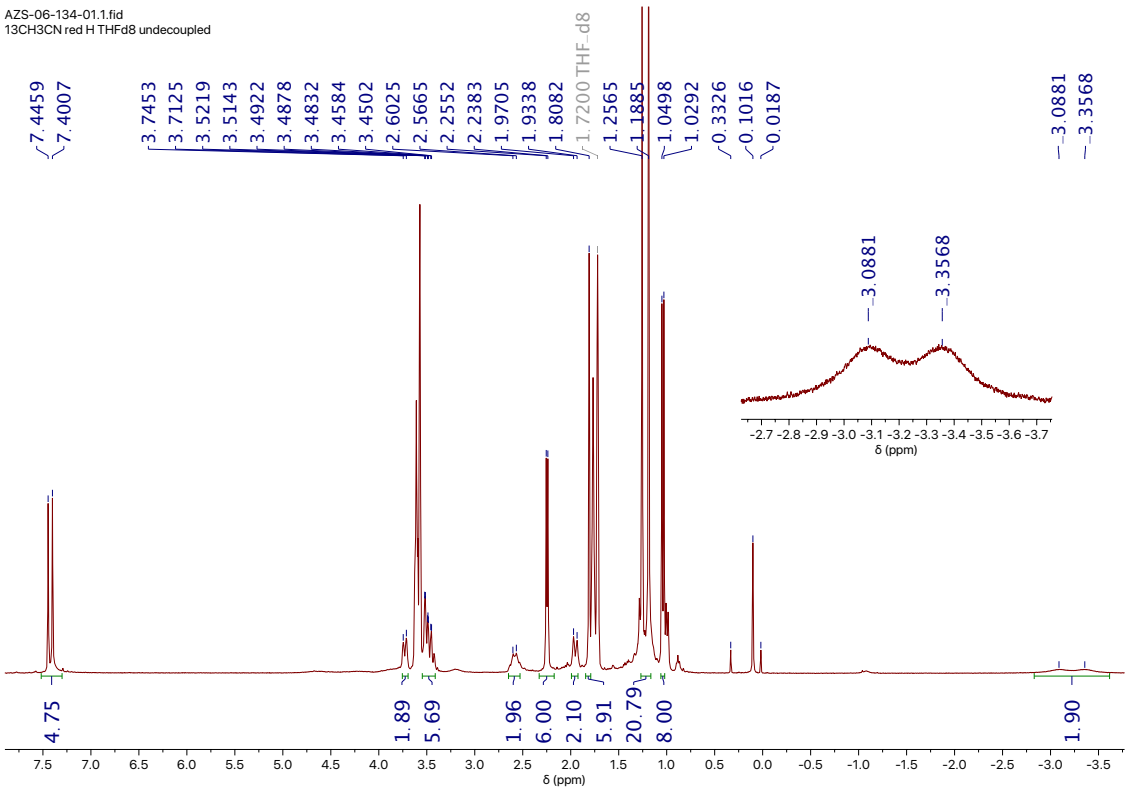

Figure S34: ^{1}H NMR spectrum of **[Co$_2$^{13}CH$_3$]$^+$** in THF-d_8 at 300 K.

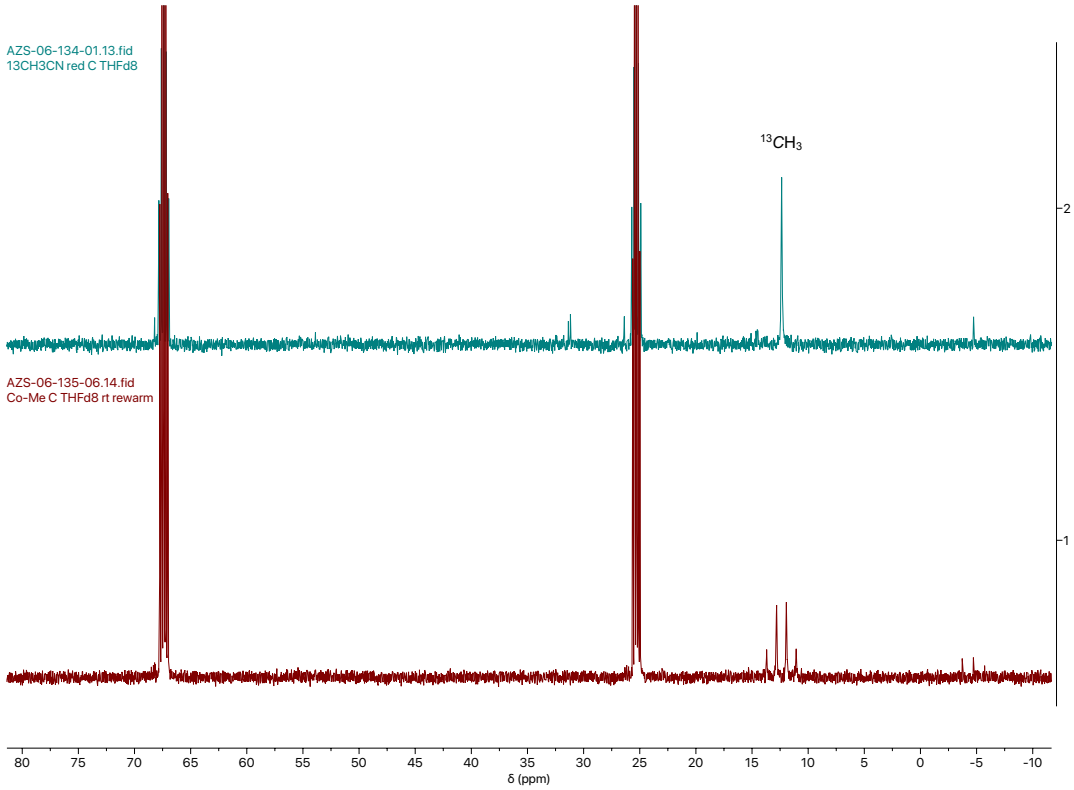

Figure S35: Top: $^{13}C\{^{1}H\}$ NMR spectrum of **[Co$_2$^{13}CH$_3$]$^+$** in THF-d_8 at 300 K. Bottom: ^{13}C NMR spectrum of **[Co$_2$^{13}CH$_3$]$^+$** in THF-d_8 at 300 K.

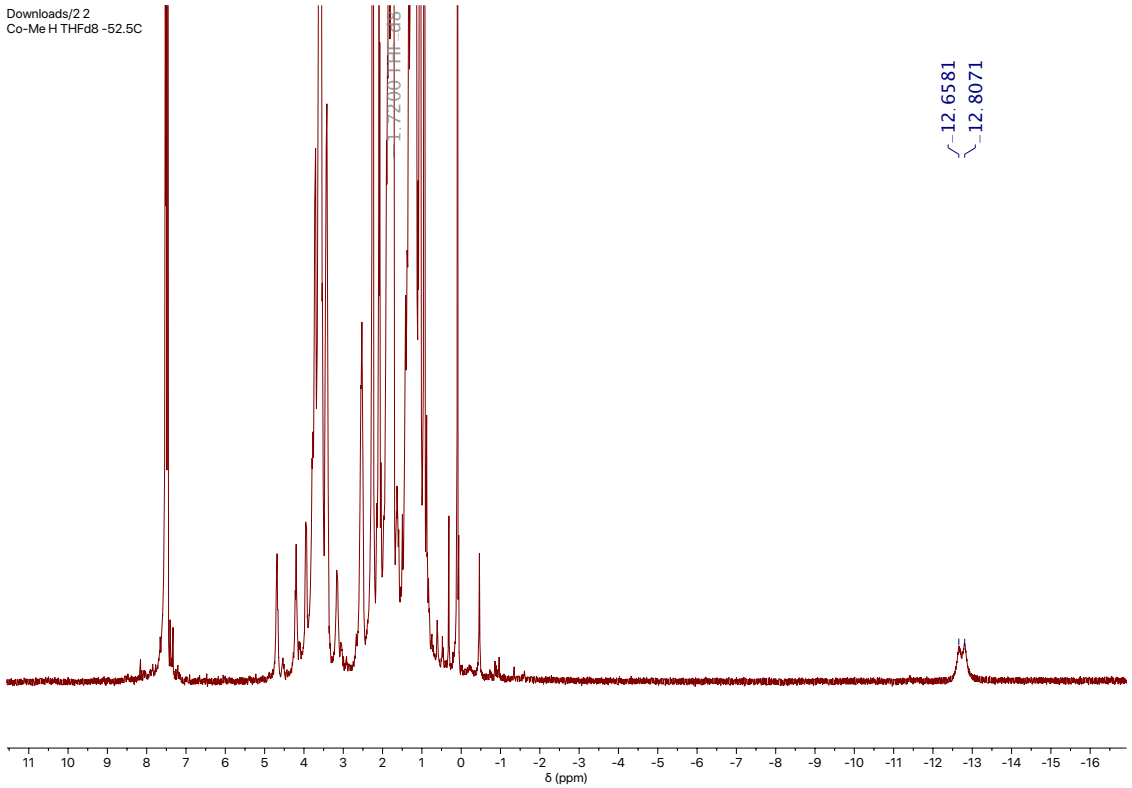

Figure S36: ^{1}H NMR spectrum of **[Co$_2$^{13}CH$_3$]$^+$** in THF-d_8 at 220 K.

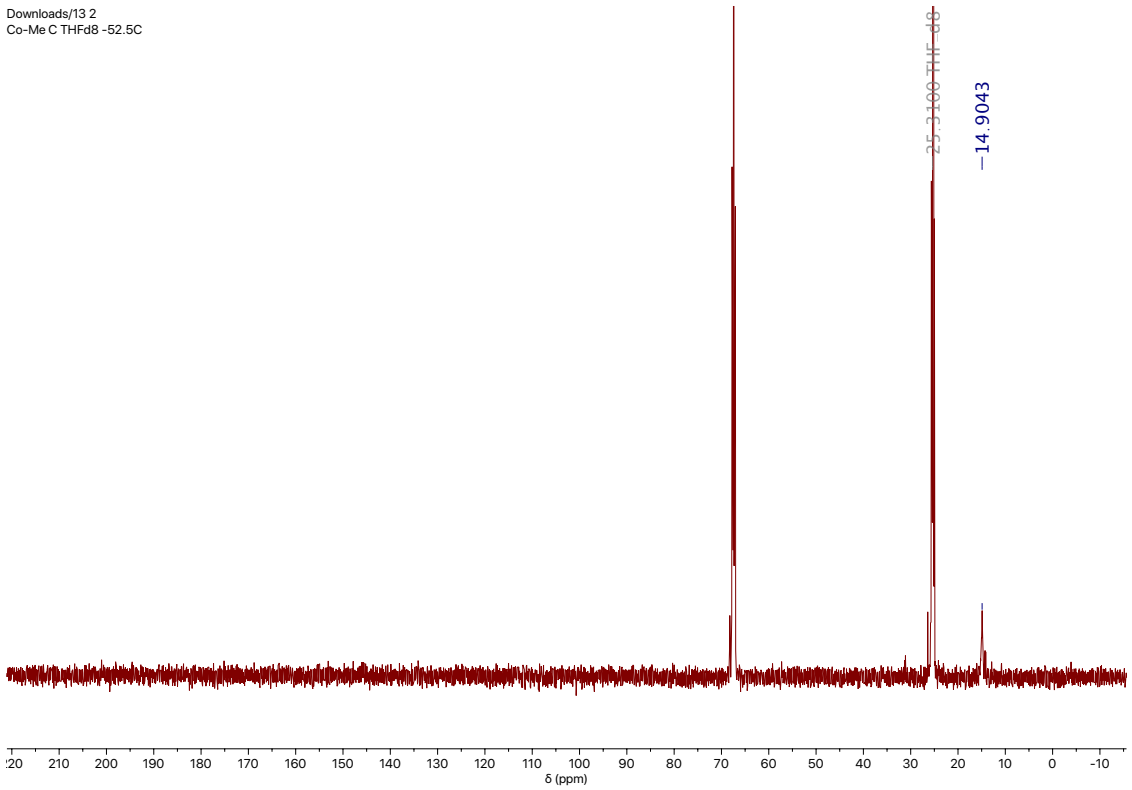

Figure S37: $^{13}C\{^{1}H\}$ NMR spectrum of $\mathbf{[Co_2{}^{13}CH_3]^+}$ in THF-d_8 at 220 K

IR Spectra

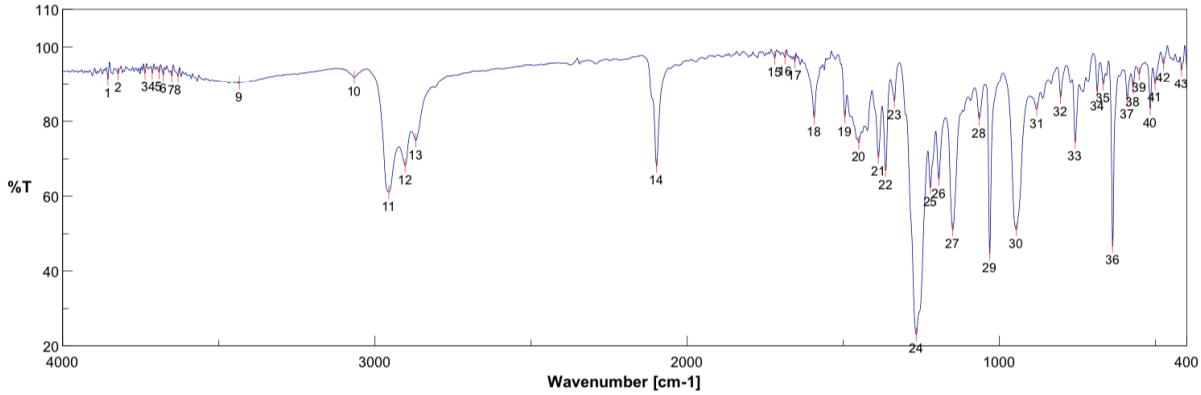

Accumulation	16	Resolution	4 cm-1
Zero Filling	ON	Apodization	Cosine
Gain	Auto (4)	Scanning Speed	Auto (2 mm/sec)
Date/Time	1/27/2020 2:08PM	Update	1/27/2020 2:09PM
Operator			
File Name	Memory#2		
Sample Name	KTO_IV_210		
Comment			

No.	cm-1	%T	No.	cm-1	%T	No.	cm-1	%T	No.	cm-1	%T	No.	cm-1	%T
1	3855.01	91.4449	2	3822.22	92.8344	3	3736.4	93.0307	4	3713.26	93.09	5	3691.09	93.1983
6	3677.59	92.5843	7	3650.59	92.2137	8	3630.34	92.1972	9	3434.6	90.3659	10	3066.26	91.8874
11	2955.38	61.0384	12	2903.31	68.1915	13	2869.56	74.8949	14	2098.17	68.0824	15	1719.23	97.0898
16	1686.44	97.2057	17	1654.62	96.1319	18	1592.91	80.9558	19	1494.56	81.178	20	1450.21	74.3462
21	1387.53	70.5218	22	1364.39	66.8785	23	1336.43	85.5147	24	1266.04	23.0617	25	1220.72	62.3883
26	1193.72	64.5861	27	1149.37	51.0571	28	1064.51	80.6801	29	1030.77	44.6601	30	945.913	51.0878
31	880.345	83.2517	32	804.171	86.5201	33	756.923	74.5136	34	686.534	87.9878	35	667.25	90.0233
36	637.358	46.7238	37	590.111	85.7778	38	571.79	89.112	39	552.506	92.7757	40	516.829	83.503
41	501.401	90.2139	42	474.403	95.5877	43	416.549	93.9142						

Figure S38: IR (KBr) spectrum of **[Co_2CN]$^+$**

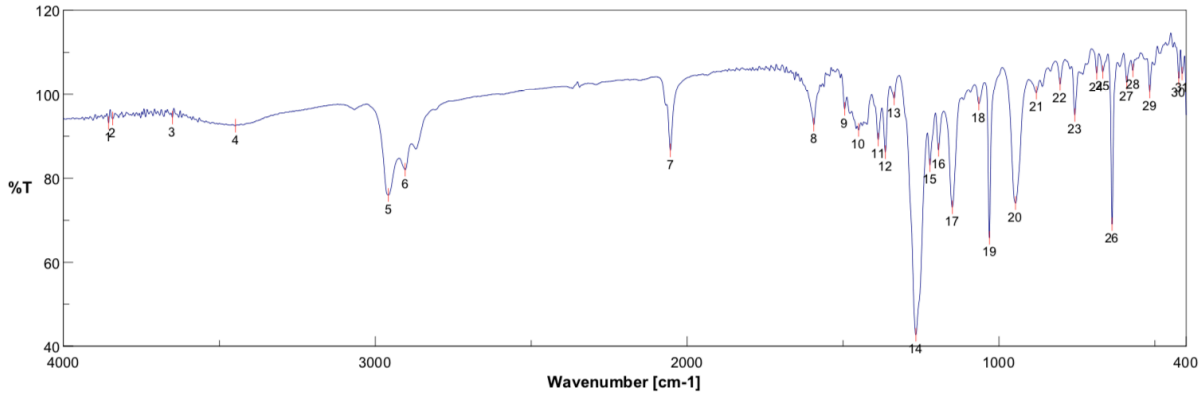

Accumulation	16	Resolution	4 cm-1
Zero Filling	ON	Apodization	Cosine
Gain	Auto (4)	Scanning Speed	Auto (2 mm/sec)
Date/Time	1/29/2020 1:13PM	Update	1/29/2020 1:14PM
Operator			
File Name	Memory#2		
Sample Name	KTO_IV_210		
Comment			

No.	cm-1	%T	No.	cm-1	%T	No.	cm-1	%T	No.	cm-1	%T	No.	cm-1	%T
1	3855.01	93.1719	2	3841.51	94.2246	3	3650.59	94.4461	4	3448.1	92.5302	5	2958.27	76.0127
6	2904.27	82.0468	7	2053.82	86.6352	8	1593.88	92.7496	9	1494.56	96.5254	10	1450.21	91.5307
11	1387.53	89.2203	12	1364.39	86.2341	13	1336.43	99.011	14	1266.04	42.7454	15	1221.68	83.1123
16	1193.72	86.7762	17	1149.37	73.0782	18	1064.51	97.7404	19	1030.77	65.8021	20	946.877	74.0867
21	880.345	100.387	22	804.171	102.437	23	756.923	95.0376	24	686.534	105.103	25	667.25	105.364
26	637.358	69.0766	27	590.111	102.81	28	570.826	105.724	29	516.829	100.659	30	423.298	103.804
31	412.692	104.99												

Figure S39: IR (KBr) spectrum of **[$Co_2{}^{13}CN$]$^+$**

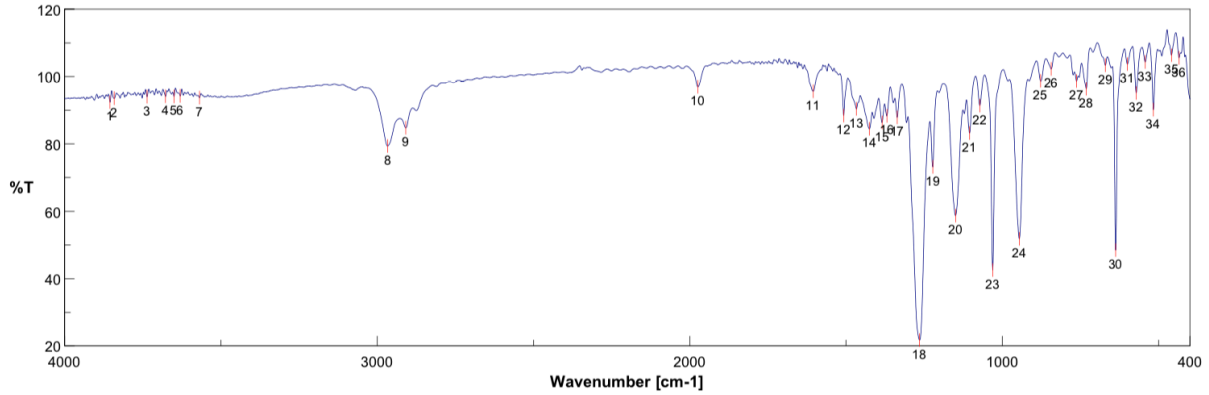

Accumulation	16	Resolution	4 cm-1
Zero Filling	ON	Apodization	Cosine
Gain	Auto (4)	Scanning Speed	Auto (2 mm/sec)
Date/Time	1/29/2020 6:27PM	Update	1/29/2020 6:27PM
Operator			
File Name	Memory#2		
Sample Name	KTO_IV_210		
Comment			

No.	cm-1	%T	No.	cm-1	%T	No.	cm-1	%T	No.	cm-1	%T	No.	cm-1	%T
1	3855.01	92.4339	2	3841.51	93.5899	3	3736.4	94.0394	4	3677.59	94.1678	5	3650.59	94.0994
6	3630.34	94.244	7	3568.63	93.724	8	2966.95	79.3988	9	2909.09	84.7725	10	1974.75	96.9619
11	1604.48	95.6444	12	1507.1	88.3803	13	1466.6	90.408	14	1425.14	84.4852	15	1384.64	86.4234
16	1369.21	88.3625	17	1336.43	87.9121	18	1265.07	21.8011	19	1222.65	73.2128	20	1149.37	58.6929
21	1105.01	83.2397	22	1072.23	91.4235	23	1030.77	42.5749	24	945.913	51.8454	25	877.452	98.7561
26	843.704	102.285	27	762.709	98.7155	28	731.853	96.4211	29	670.142	103.408	30	637.358	48.4623
31	599.753	103.755	32	571.79	95.1243	33	542.863	104.371	34	516.829	90.2147	35	458.975	106.411
36	434.869	105.589												

Figure S40: IR (KBr) spectrum of **$[Co_2CN]^{2+}$**

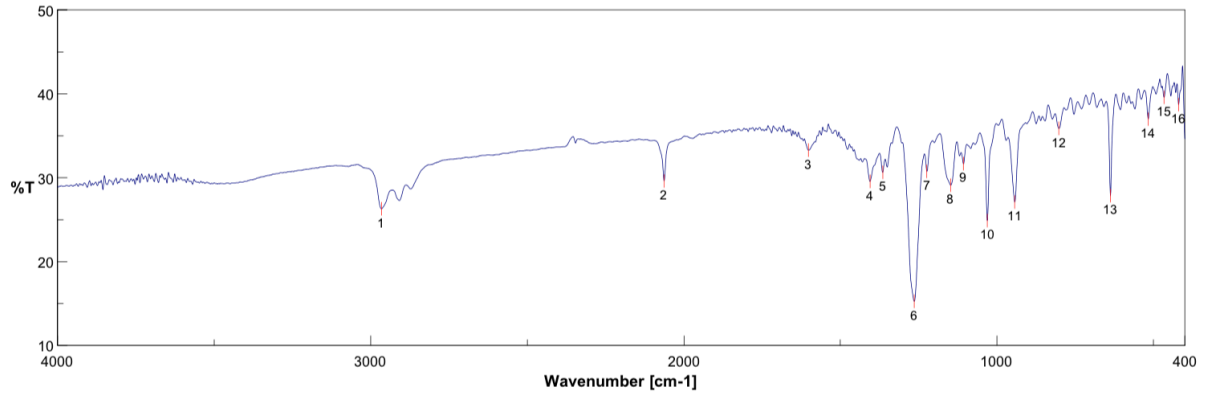

Accumulation	16	Resolution	4 cm-1
Zero Filling	ON	Apodization	Cosine
Gain	Auto (4)	Scanning Speed	Auto (2 mm/sec)
Date/Time	2/3/2020 3:32PM	Update	2/3/2020 3:35PM
Operator			
File Name	Memory#2		
Sample Name	KTO_IV_210		
Comment			

No.	cm-1	%T	No.	cm-1	%T	No.	cm-1	%T	No.	cm-1	%T	No.	cm-1	%T
1	2965.98	26.3106	2	2063.46	29.6179	3	1601.59	33.287	4	1404.89	29.5842	5	1364.39	30.6439
6	1264.11	15.2932	7	1223.61	30.7697	8	1147.44	29.1181	9	1106.94	31.689	10	1030.77	24.909
11	943.02	27.116	12	802.242	35.8877	13	637.358	27.864	14	516.829	37.0007	15	466.689	39.5919
16	419.442	38.7092												

Figure S41: IR (KBr) spectrum of **$[Co_4(CN)_2][OTf]_2$**.

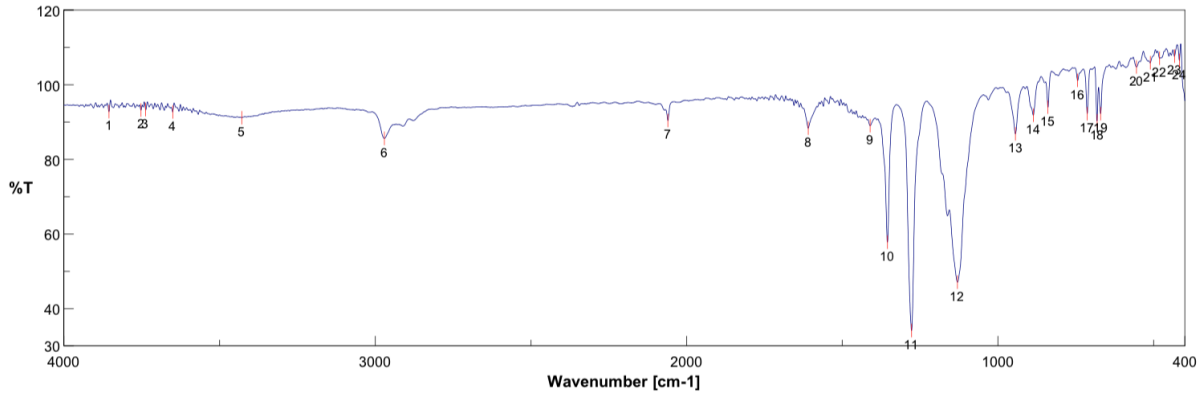

Accumulation	16	Resolution	4 cm-1
Zero Filling	ON	Apodization	Cosine
Gain	Auto (4)	Scanning Speed	Auto (2 mm/sec)
Date/Time	1/27/2020 3:24PM	Update	1/27/2020 3:24PM
Operator			
File Name	Memory#3		
Sample Name	KTO_IV_210		
Comment			

No.	cm-1	%T	No.	cm-1	%T	No.	cm-1	%T	No.	cm-1	%T	No.	cm-1	%T
1	3855.01	92.8181	2	3752.8	93.2155	3	3737.37	93.3049	4	3650.59	92.7151	5	3428.81	91.1794
6	2970.8	85.632	7	2060.57	90.4411	8	1609.31	88.382	9	1410.67	89.0275	10	1354.75	57.8
11	1277.61	34.1205	12	1130.08	47.1035	13	943.985	86.8431	14	886.131	91.813	15	839.847	94.0219
16	744.388	101.206	17	713.533	92.2652	18	681.713	90.3157	19	670.142	92.251	20	555.398	104.777
21	511.044	105.94	22	481.153	107.111	23	432.941	107.679	24	417.513	106.552			

Figure S42: IR (KBr) spectrum of **$[Co_4(CN)_2][BAr^F{}_4]_2$**.

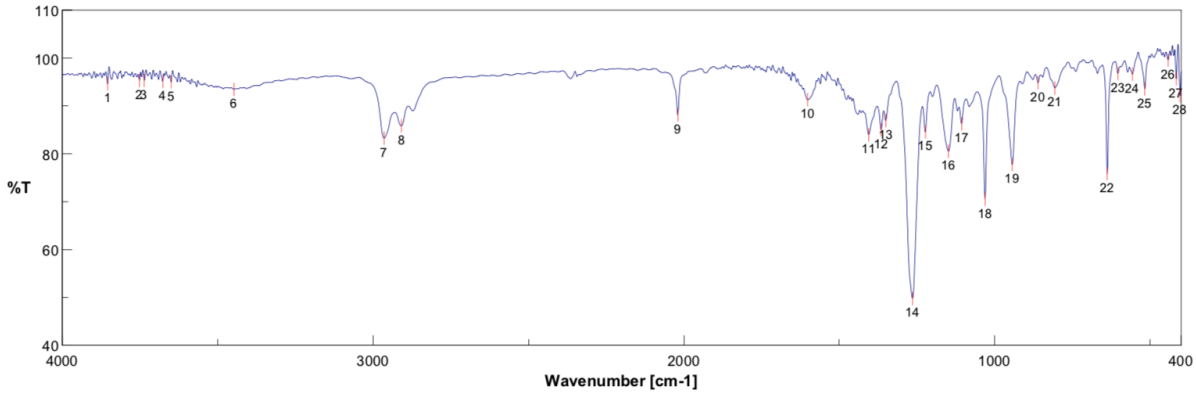

Accumulation	16	Resolution	4 cm-1
Zero Filling	ON	Apodization	Cosine
Gain	Auto (4)	Scanning Speed	Auto (2 mm/sec)
Date/Time	1/29/2020 7:22PM	Update	1/29/2020 7:23PM
Operator			
File Name	Memory#3		
Sample Name	KTO_IV_210		
Comment			

No.	cm-1	%T	No.	cm-1	%T	No.	cm-1	%T	No.	cm-1	%T	No.	cm-1	%T
1	3854.04	94.6549	2	3751.83	95.3183	3	3736.4	95.355	4	3676.62	95.1655	5	3649.62	95.0238
6	3448.1	93.4653	7	2965.02	83.2494	8	2909.09	85.8394	9	2020.07	88.1241	10	1601.59	91.3123
11	1404.89	83.9995	12	1365.35	85.0299	13	1349.93	86.9212	14	1264.11	49.7839	15	1222.65	84.58
16	1148.4	80.5351	17	1105.98	86.2461	18	1030.77	70.53	19	943.02	77.8121	20	860.096	94.8645
21	806.099	93.7758	22	637.358	75.8632	23	603.61	96.8103	24	556.363	96.6619	25	516.829	93.5658
26	441.619	99.6299	27	415.585	95.7047	28	403.05	92.0879						

Figure S43: IR (KBr) spectrum of **$[Co_4{}^{13}CN_2][OTf]_2$**.

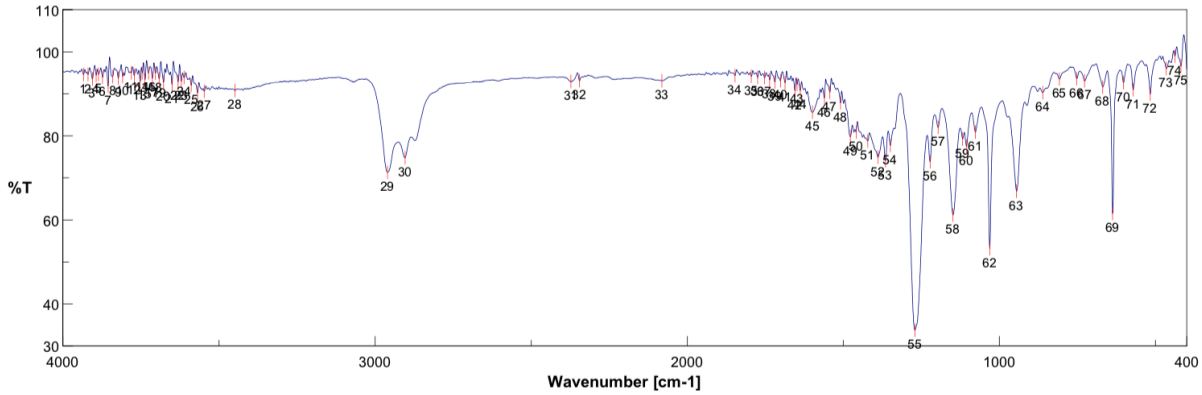

Accumulation	16	Resolution	4 cm-1
Zero Filling	ON	Apodization	Cosine
Gain	Auto (4)	Scanning Speed	Auto (2 mm/sec)
Date/Time	3/14/2020 7:41PM	Update	3/14/2020 7:43PM
Operator			
File Name	Memory#1		
Sample Name	KTO_IV_191		
Comment			

No.	cm-1	%T	No.	cm-1	%T	No.	cm-1	%T	No.	cm-1	%T	No.	cm-1	%T
1	3934.07	94.6007	2	3919.61	94.6149	3	3905.15	93.5321	4	3893.57	94.4479	5	3885.86	94.6501
6	3873.33	93.9543	7	3855.01	91.8596	8	3840.54	94.118	9	3822.22	93.7219	10	3808.72	94.1836
11	3780.76	95.0372	12	3771.12	94.3943	13	3752.8	92.9515	14	3746.05	95.0187	15	3737.37	93.365
16	3725.8	94.9974	17	3713.26	93.7469	18	3703.62	94.9403	19	3692.05	93.6164	20	3677.59	92.8017
21	3650.59	92.1502	22	3631.3	92.9733	23	3620.7	93.0273	24	3612.02	93.916	25	3588.88	92.0286
26	3568.63	90.2521	27	3547.41	90.6147	28	3449.06	90.7729	29	2960.2	71.3495	30	2904.27	74.7918
31	2372.98	92.9713	32	2345.98	93.1141	33	2081.78	93.1449	34	1846.51	94.3847	35	1794.44	94.1729
36	1774.19	93.9371	37	1752.01	93.8714	38	1735.62	93.3663	39	1719.23	92.8667	40	1700.91	93.1537
41	1686.44	92.6216	42	1654.62	90.7684	43	1647.87	92.266	44	1637.27	90.8087	45	1598.7	85.6369
46	1560.13	89.0236	47	1542.77	90.3996	48	1509.03	87.8667	49	1477.21	79.8487	50	1458.89	80.9123
51	1421.28	78.8203	52	1388.5	74.8941	53	1364.39	74.1117	54	1348.96	77.7592	55	1270.86	33.789
56	1221.68	73.8727	57	1196.61	81.9992	58	1148.4	61.2129	59	1117.55	79.2705	60	1105.01	77.5636

Figure S44: IR (KBr) spectrum of **[Co_2CH_3]$^+$**

UV-Vis Spectra

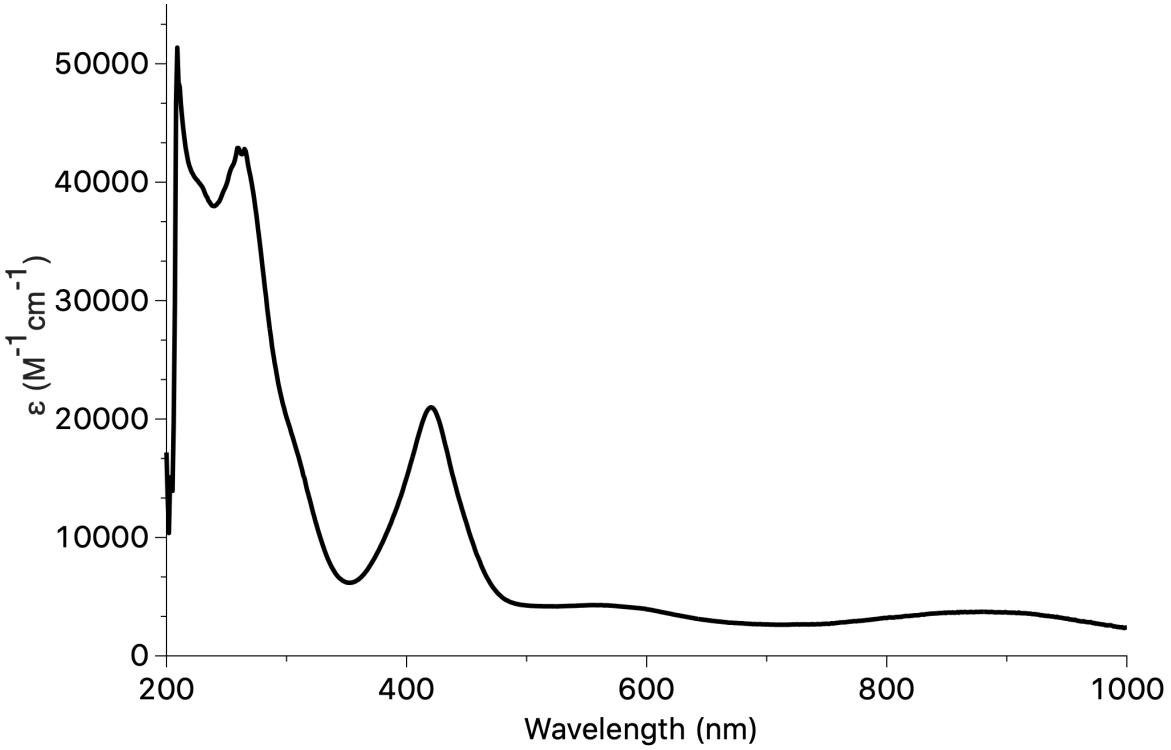

Figure S45: UV-Vis spectrum of **[Co_2CN]**$^+$ in THF. The intense feature at 265 nm is observed across previously characterized ^{3}PDI$_2$ macrocyclic systems[1] and is assigned as a ligand π→π* transition. The lower energy absorptions between 400 and 600 nm are similarly observed in the isoelectronic **[Co_2Cl]**$^+$ complex and are assigned as MLCT transitions.

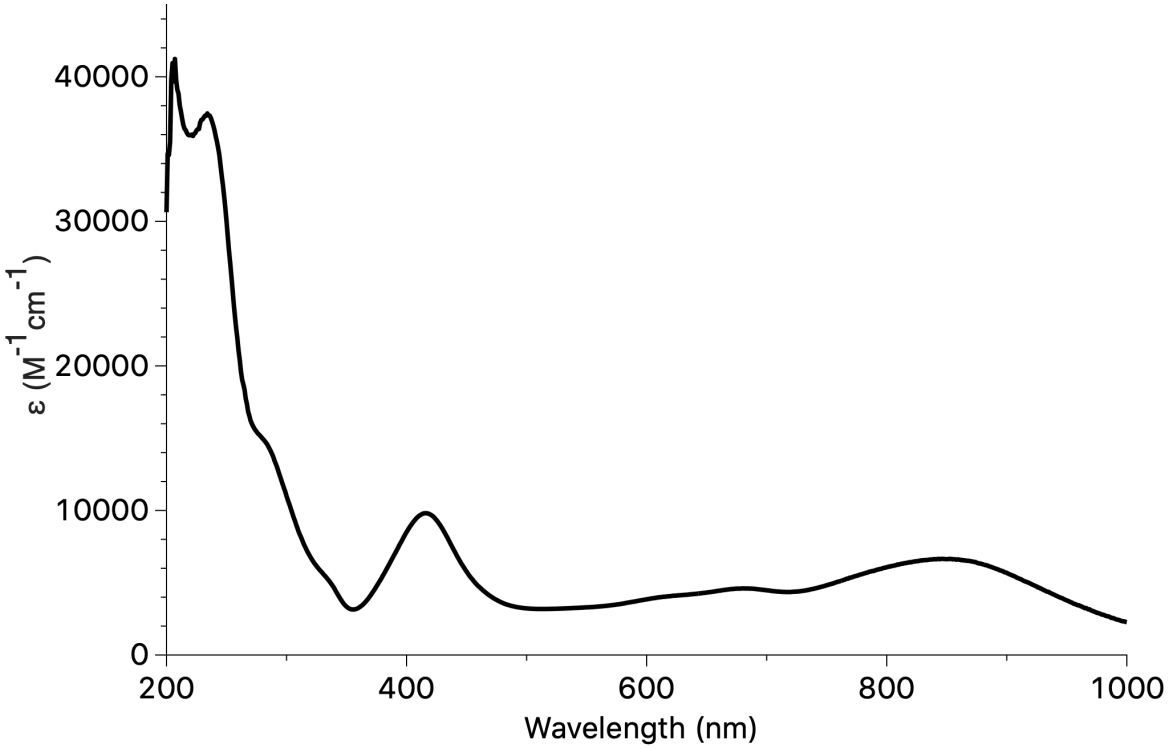

Figure S46: UV-Vis spectrum of **[Co_2CN]**$^{2+}$ in MeCN.

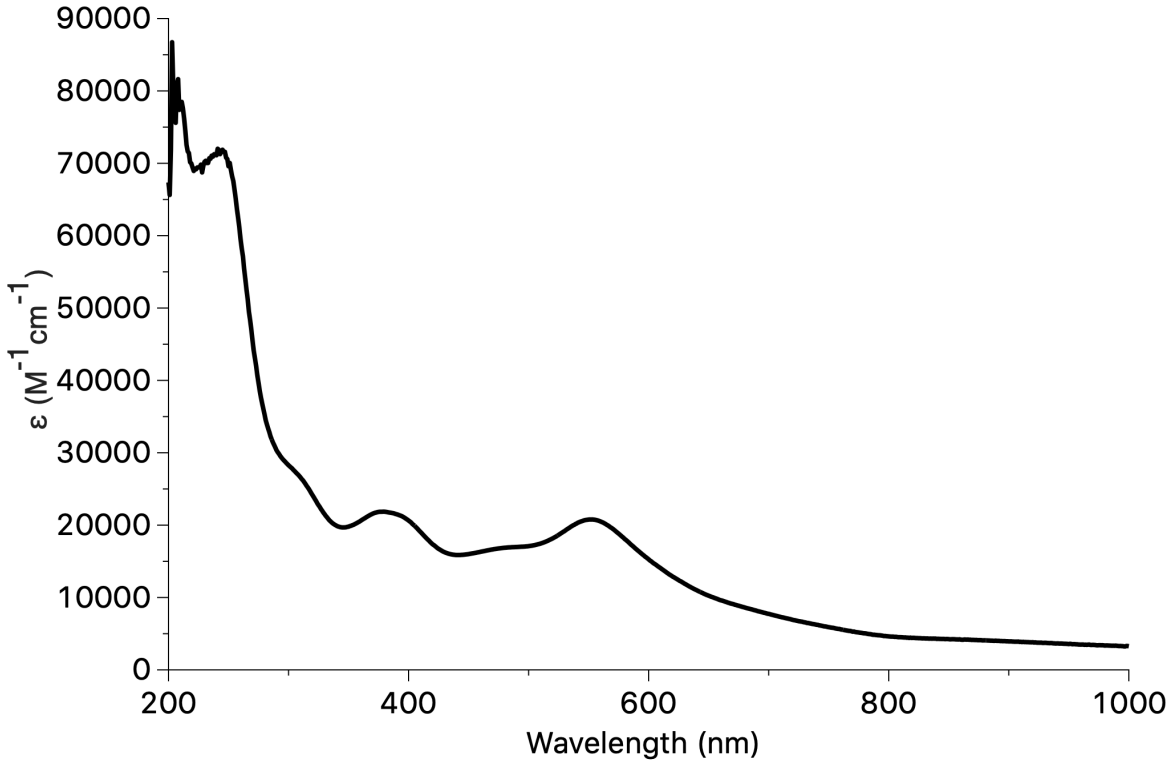

Figure S47: UV-Vis spectrum of **[$Co_4(CN)_2$][OTf]$_2$** in MeCN.

Cyclic Voltammogram

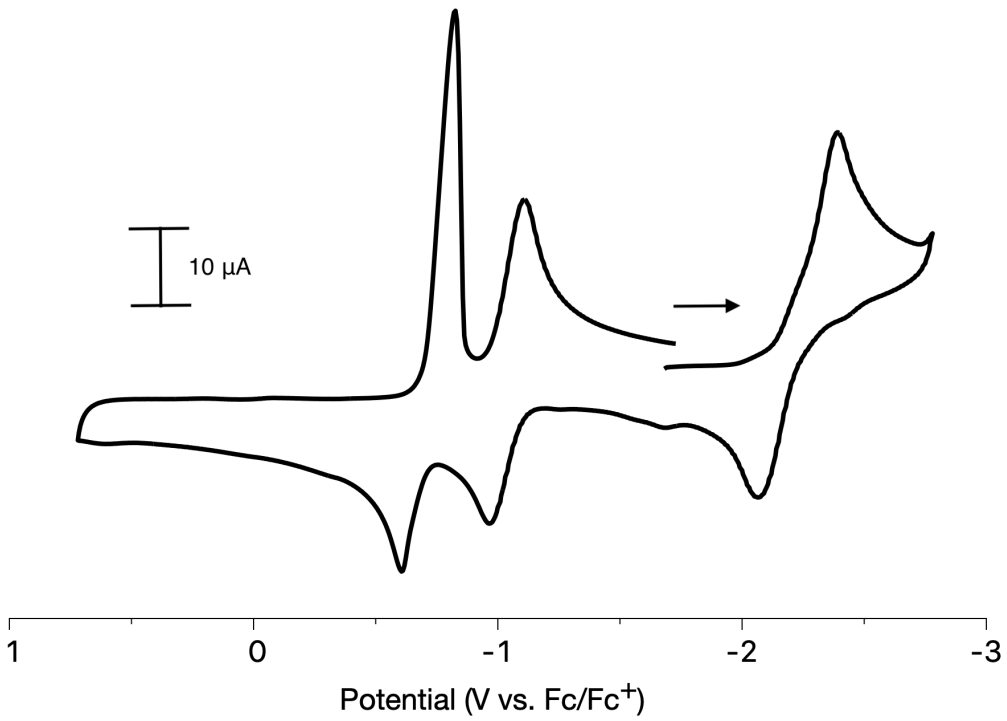

Figure S48: Cyclic voltammogram of **[Co_2CN]**$^+$ in 1,2-difluorobenzene at 100 mV/s. Conditions: 1 mM of analyte in 0.1 M [^{n}Bu$_4$N][PF$_6$] in 1,2-difluorobenzene, glassy carbon working electrode, Pt auxiliary electrode, 0.1 M AgBAr$^F{}_4$/Ag reference electrode.

X-ray Crystallography

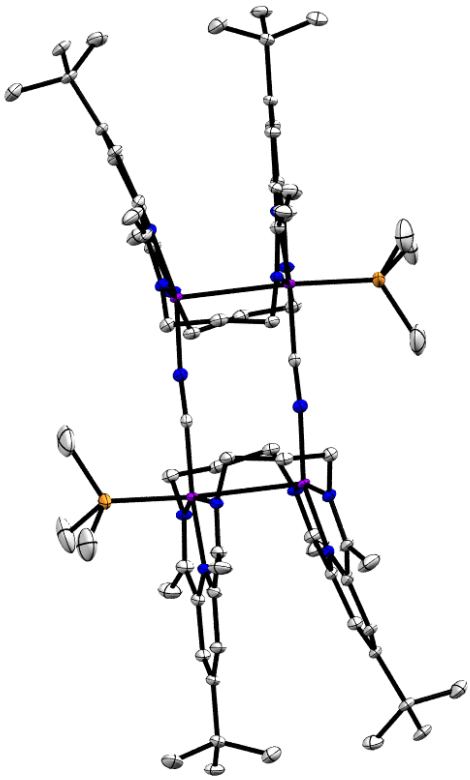

Figure S49: X-ray structure of cationic portion of **[$Co_4(CN)_2$][OTf]$_2$**. Hydrogen atoms and ambiguous/disordered triflates were removed for clarity.

Table S1: Summary of Structure Determination of Compound $[Co_2CH_3]^+$

Empirical formula	$C_{48}H_{75}Co_2F_4N_6O_3PS$
Formula weight	1041.03
Temperature/K	100
Crystal system	monoclinic
Space group	$P2_1/n$
a	11.1401(12)Å
b	18.761(2)Å
c	26.561(3)Å
β	90.032(6)°
Volume	5551.2(10)Å^3
Z	4
d_{calc}	1.246 g/cm^3
μ	0.719 mm^{-1}
F(000)	2200.0
Crystal size, mm	0.5 × 0.12 × 0.03
2θ range for data collection	2.658 - 55.078°
Index ranges	$-13 \leq h \leq 14$, $-24 \leq k \leq 24$, $-34 \leq l \leq 34$
Reflections collected	120138
Independent reflections	12780[R(int) = 0.0516]
Data/restraints/parameters	12780/0/570
Goodness-of-fit on F^2	1.029
Final R indexes [I>=2σ (I)]	R_1 = 0.0496, wR_2 = 0.1284
Final R indexes [all data]	R_1 = 0.0578, wR_2 = 0.1335
Largest diff. peak/hole	0.98/-1.23 eÅ^{-3}

Table S2: Summary of Structure Determination of Compound $[Co_2CN]^+$

Empirical formula	$C_{97}H_{150}Co_4F_8N_{14}O_6P_4S_2$
Formula weight	2184.02
Temperature/K	100
Crystal system	monoclinic
Space group	Cm
a	22.620(4)Å
b	21.110(4)Å
c	12.650(2)Å
β	115.833(5)°
Volume	5436.8(17)Å^3
Z	2
d_{calc}	1.334 g/cm^3
μ	0.766 mm^{-1}
F(000)	2300.0
Crystal size, mm	0.45 × 0.1 × 0.08
2θ range for data collection	2.78 - 55.16°
Index ranges	$-29 \leq h \leq 29$, $-27 \leq k \leq 27$, $-16 \leq l \leq 10$
Reflections collected	82772
Independent reflections	10823[R(int) = 0.0371]
Data/restraints/parameters	10823/287/748
Goodness-of-fit on F^2	1.023
Final R indexes [I>=2σ (I)]	R_1 = 0.0354, wR_2 = 0.0892
Final R indexes [all data]	R_1 = 0.0387, wR_2 = 0.0912
Largest diff. peak/hole	0.88/-0.50 eÅ^{-3}
Flack parameter	0.004(3)

Table S3: Summary of Structure Determination of Compound $[Co_2CN]^{2+}$

Empirical formula	$C_{41}H_{64}Co_2F_6N_7O_6P_2S_2$
Formula weight	1108.91
Diffractometer	Rigaku XtaLAB Synergy-S (Dectris Pilatus3 R 200K)
Temperature/K	100
Crystal system	monoclinic
Space group	C2/c
a	20.5654(6)Å
b	12.3627(3)Å
c	20.3762(6)Å
β	108.773(3)°
Volume	4904.9(2)Å^3
Z	4
d_{calc}	1.502 g/cm^3
μ	0.902 mm^{-1}
F(000)	2308.0
Crystal size, mm	0.68 × 0.23 × 0.2
2θ range for data collection	4.184 - 54.962°
Index ranges	$-24 \leq h \leq 26$, $-15 \leq k \leq 16$, $-26 \leq l \leq 26$
Reflections collected	45191
Independent reflections	5619[R(int) = 0.0486]
Data/restraints/parameters	5619/6/315
Goodness-of-fit on F^2	1.056
Final R indexes [I>=2σ (I)]	R_1 = 0.0378, wR_2 = 0.1004
Final R indexes [all data]	R_1 = 0.0418, wR_2 = 0.1024
Largest diff. peak/hole	2.04/-0.43 eÅ^{-3}

Table S4: Summary of Structure Determination of Compound $[Co_4(CN)_2][BAr^F{}_4]_2$

Empirical formula	$C_{136}H_{134}B_2Co_4F_{48}N_{14}P_2$
Formula weight	3195.84
Temperature/K	100
Crystal system	orthorhombic
Space group	$C222_1$
a	10.4664(6)Å
b	35.353(2)Å
c	39.212(2)Å
Volume	14509.3(15)Å^3
Z	4
d_{calc}	1.463 g/cm^3
μ	0.586 mm^{-1}
F(000)	6512.0
Crystal size, mm	0.5 × 0.12 × 0.02
2θ range for data collection	5.118 - 55.052°
Index ranges	$-13 \leq h \leq 13$, $-45 \leq k \leq 45$, $-50 \leq l \leq 50$
Reflections collected	128906
Independent reflections	16697[R(int) = 0.1138]
Data/restraints/parameters	16697/5487/1824
Goodness-of-fit on F^2	1.048
Final R indexes [I>=2σ (I)]	R_1 = 0.0692, wR_2 = 0.1677
Final R indexes [all data]	R_1 = 0.0988, wR_2 = 0.1885
Largest diff. peak/hole	1.01/-0.64 eÅ^{-3}
Flack parameter	0.32(2)

Table S5: Summary of Structure Determination of Compound $[Co_4(CN)_2][OTf]_2$

Empirical formula	$C_{72}H_{110}Co_4N_{14}P_2$
Formula weight	1469.39
Temperature/K	100
Crystal system	monoclinic
Space group	P2/n
a	10.0438(18)Å
b	10.802(2)Å
c	42.393(8)Å
β	91.568(5)°
Volume	4597.4(14)Å^3
Z	2
d_{calc}	1.061 g/cm^3
μ	0.784 mm^{-1}
F(000)	1556.0
Crystal size, mm	0.3 × 0.15 × 0.12
2θ range for data collection	5.828 - 55.124°
Index ranges	$-13 \leq h \leq 13$, $-14 \leq k \leq 14$, $-55 \leq l \leq 55$
Reflections collected	164721
Independent reflections	10575[R(int) = 0.0848]
Data/restraints/parameters	10575/72/458
Goodness-of-fit on F^2	1.094
Final R indexes [I>=2σ (I)]	R_1 = 0.0622, wR_2 = 0.1401
Final R indexes [all data]	R_1 = 0.0823, wR_2 = 0.1496
Largest diff. peak/hole	1.02/-0.73 eÅ^{-3}

References

1. Q. Wang, S. Zhang, P. Cui, A. B. Weberg, L. M. Thierer, B. C. Manor, M. R. Gau, P. J. Carroll and N. C. Tomson, *Inorg. Chem.*, 2020, **59**, 4200–4214.
2. M. A. Schwindt, T. Lejon and L. S. Hegedus, *Organometallics*, 1990, **9**, 2814–2819.
3. M. L. Luetkens, A. P. Sattelberger, H. H. Murray, J. D. Basil, J. P. Fackler, R. A. Jones and D. E. Heaton, in *Inorg. Synth.*, John Wiley & Sons, Ltd, 2007, pp. 305–310.
4. N. A. Yakelis and R. G. Bergman, *Organometallics*, 2005, **24**, 3579–3581.
5. B. E. Love and E. G. Jones, *J. Org. Chem.*, 1999, **64**, 3755–3756.
6. C. Zoski, *Handbook of Electrochemistry*, Elsevier Science, Amsterdam, 2007.
7. L. Kaplan, W. L. Kester and J. J. Katz, *J. Am. Chem. Soc.*, 1952, **74**, 5531–5532.
8. C. P. Rosenau, B. J. Jelier, A. D. Gossert and A. Togni, *Angew. Chem. Int. Ed.*, 2018, **57**, 9528–9533.
9. D. F. Evans, *J. Chem. Soc.*, 1959, 2003–2005.
10. Bruker SAINT v8.38A; Bruker AXS Inc.: Madison, WI, 2014.
11. CrysAlisPro 1.171.40.53: Rigaku Oxford Diffraction, Rigaku Corporation, Oxford, UK, 2019.
12. L. Krause, R. Herbst-Irmer, G. M. Sheldrick and D. Stalke, *J. Appl. Crystallogr.*, 2015, **48**, 3–10.
13. SCALE3 ABSPACK v1.0.7: An Oxford Diffraction Program; Oxford Diffraction Ltd: Abingdon, UK, 2005.
14. G. M. Sheldrick, *Acta Crystallogr., Sect. A: Found. Crystallogr.*, 2015, **71**, 3–8.
15. G. M. Sheldrick, *Acta Crystallogr., Sect. A: Found. Crystallogr.*, 2008, **64**, 112–122.
16. G. M. Sheldrick, *Acta Crystallogr., Sect. C: Struct. Chem.*, 2015, **71**, 3–8.
17. A. L. Spek, *Acta Crystallogr., Sect. C: Struct. Chem.*, 2015, **71**, 9–18.